

# The Reactivity of Air-Stable Pyridine- and Pyrimidine-Containing Diarylamine Antioxidants

Jason J. Hanthorn,<sup>†</sup> Riccardo Amorati,<sup>§</sup> Luca Valgimigli<sup>§,\*</sup> and Derek A. Pratt<sup>†,‡,\*</sup>

<sup>†</sup>Department of Chemistry, Queen's University, 90 Bader Lane, Kingston, Ontario, Canada K7L 3N6

<sup>§</sup>Department of Organic Chemistry "A. Mangini", University of Bologna, 40126, Bologna, Italy

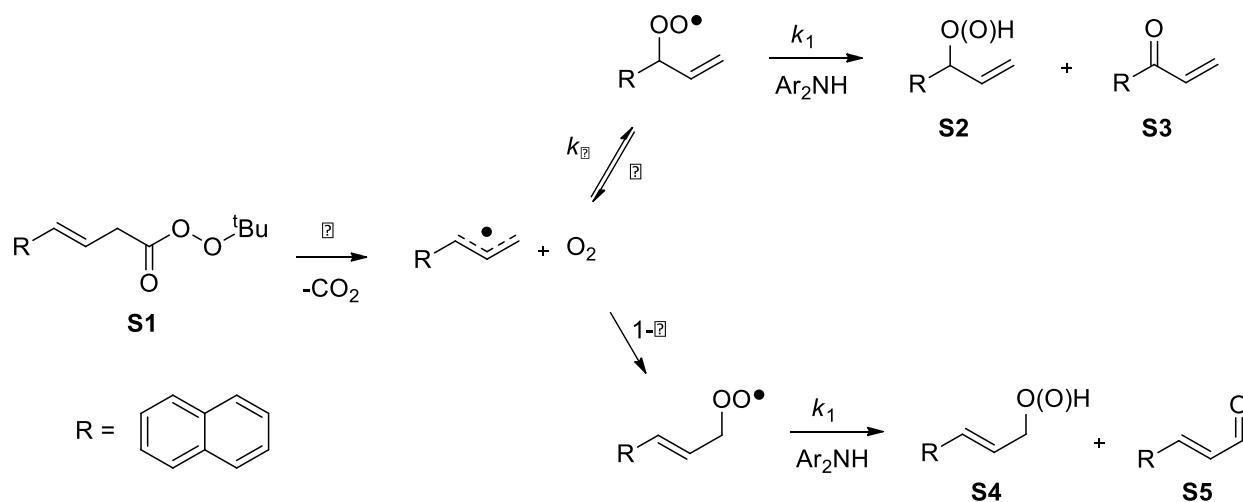
<sup>‡</sup>Department of Chemistry, University of Ottawa, Ottawa, Ontario, Canada K1N 6N5

## Supporting Information

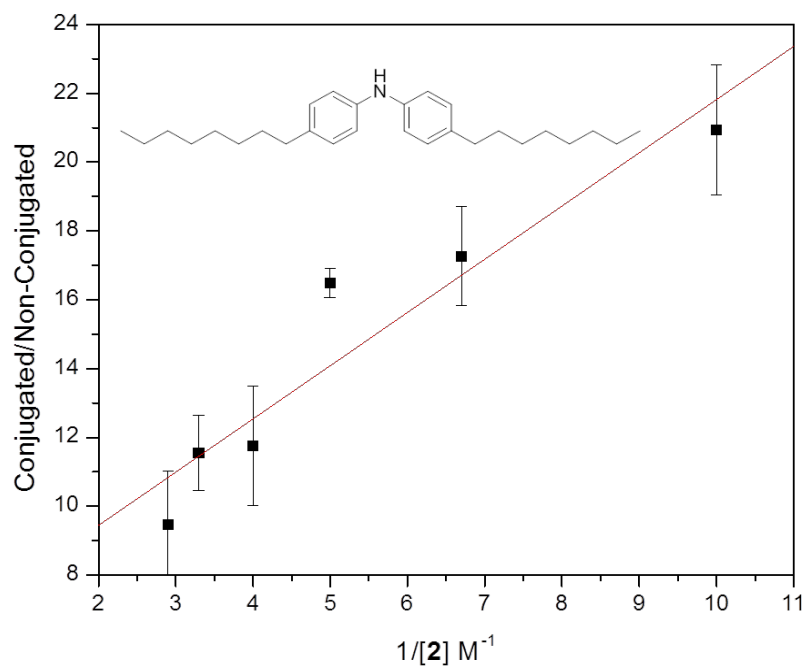
Peroxyl Radical Kinetics.....	2
Scheme 1. Peroxyester Kinetic Scheme.....	2
Figures S1-S25. Raw Data from Clocking Experiments.....	3-15
Voltammetry Experiments.....	15
Figures S26-S30. Differential Pulse Voltammograms for <b>2</b> and <b>7-11</b> .....	16-18
Figures S31-S36. Cyclic Voltammograms for <b>3</b> and <b>12-16</b> .....	19-21
Figures S37-S40. Differential Pulse Voltammograms for <b>17-21</b> .....	22-24
Figures S41-S45. Cyclic Voltammograms for <b>22-26</b> .....	24-26
Figures S46-S50. Differential Pulse Voltammograms for <b>27-31</b> .....	26-29
Figures S51-S52. Cyclic Voltammograms for <b>33-34</b> .....	29-30
Alkyl Radical Kinetics.....	30
Figures S53-S59. Raw Data from Alkyl Radical Clock Experiments.....	31-34
BDE Measurements .....	34
Table S1. EPR radical equilibrations.....	35
Figures S60-S62. Sample EPR spectra.....	36-38
References.....	39

## Peroxyl Radical Kinetics

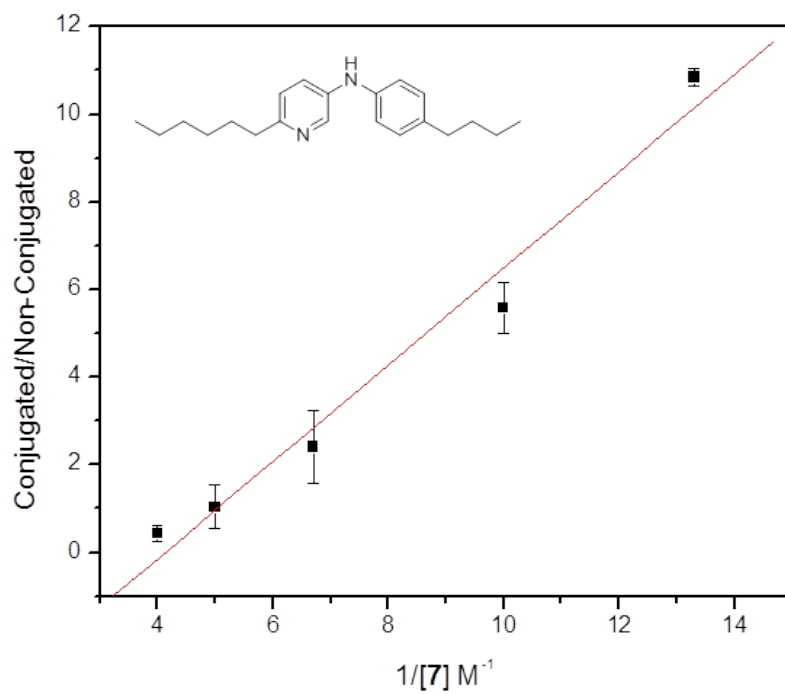
To a screw-capped GC vial was added peroxyester **S1** (0.01 M final conc.), H-atom donor (0.02 – 0.2 M final concentration, depending on  $k_H$ ) and the desired solvent to a total volume of 100  $\mu\text{L}$ . The samples were incubated at the appropriate temperature in a sand bath for 2-14 hours (depending on temperature), quenched with 100  $\mu\text{L}$  of 1 M  $\text{PPh}_3$  and diluted to 1 mL with acetonitrile for analysis. GC analysis was carried out using an Agilent DB-5 column (30 m x 0.32  $\mu\text{m}$  x 0.25  $\mu\text{m}$ ) with the following temperature profile: 130°C hold 5 min, 2°C/min to 162°C, 30°C/min to 280°C, hold 5 min. Response factors for the non-conjugated alcohol **S2**, non-conjugated ketone **S3**, conjugated alcohol **S4** and conjugated aldehyde **S5** are 1.85, 1.25, 1.21 and 1.83 respectively relative to benzyl alcohol. A plot of  $([\text{S4}] + [\text{S5}]) / ([\text{S2}] + [\text{S3}])$  (conjugated/non-conjugated) vs.  $1/[\text{H-atom donor}]$  was fit linearly to obtain  $k_H$ .<sup>1</sup>



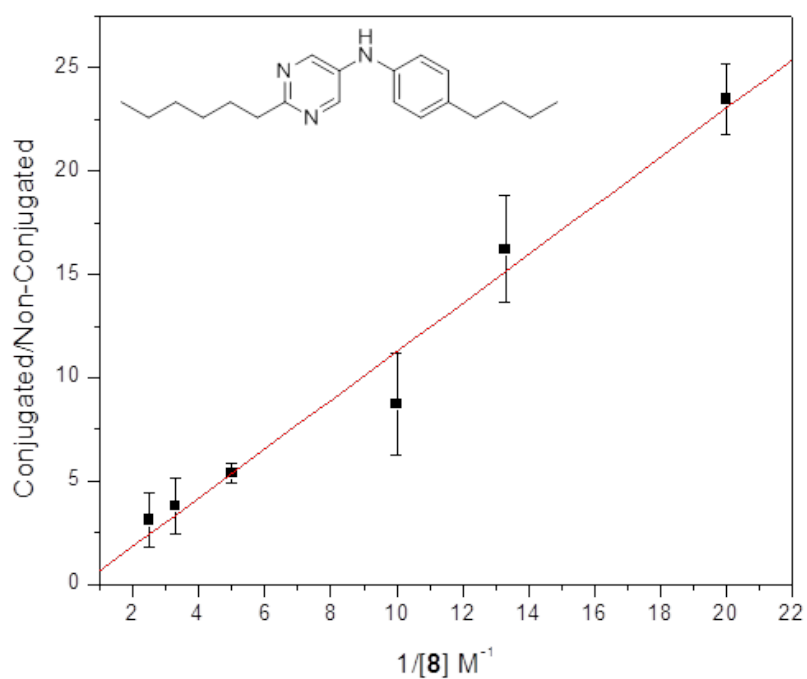
**Scheme S1.** Kinetic scheme used to determine  $k_H$  where  $k_{\beta}$  represents the known rate of  $\beta$ -fragmentation and  $\alpha$  represents the known oxygen partition coefficient.



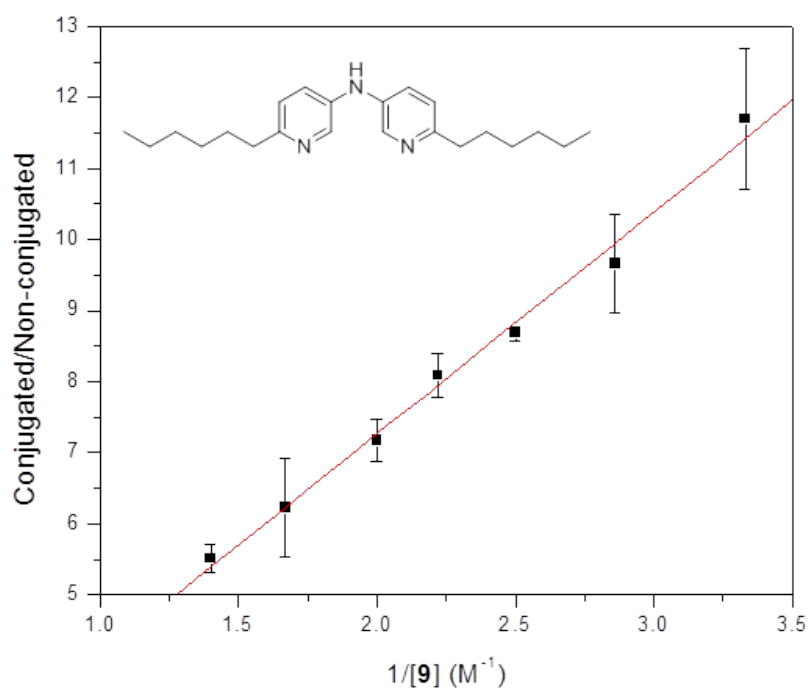
**Figure S1.** Double reciprocal plot used to obtain  $k_1 = 1.8 \times 10^5 \text{ M}^{-1}\text{s}^{-1}$  for compound 2.



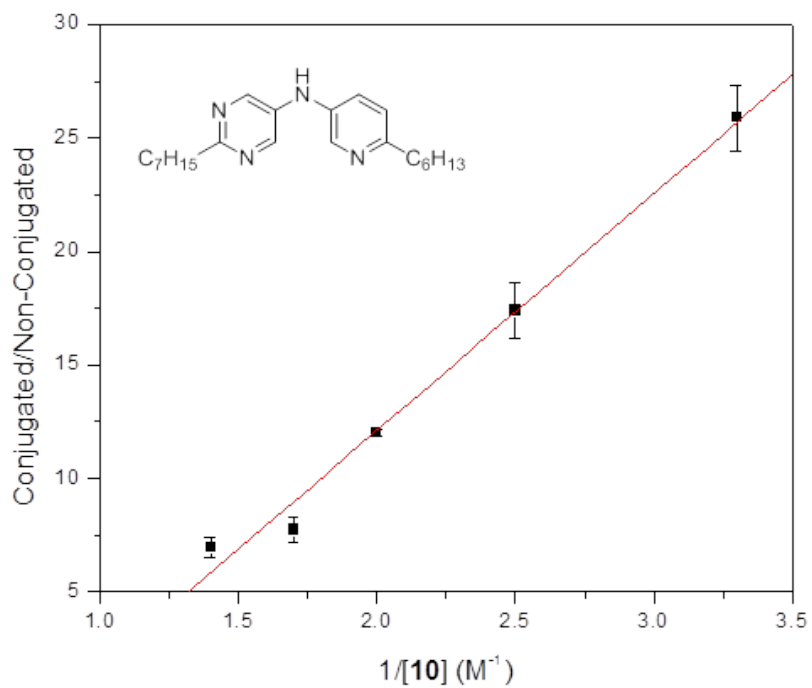
**Figure S2.** Double reciprocal plot used to obtain  $k_1 = 1.5 \times 10^5 \text{ M}^{-1}\text{s}^{-1}$  for compound 7.



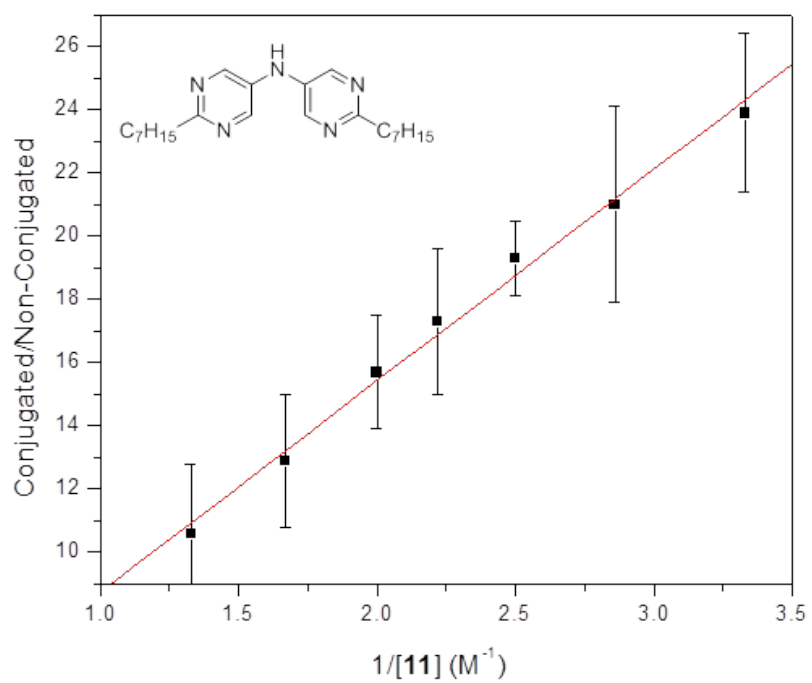
**Figure S3.** Double reciprocal plot used to obtain  $k_1 = 1.5 \times 10^5 \text{ M}^{-1}\text{s}^{-1}$  for compound **8**.



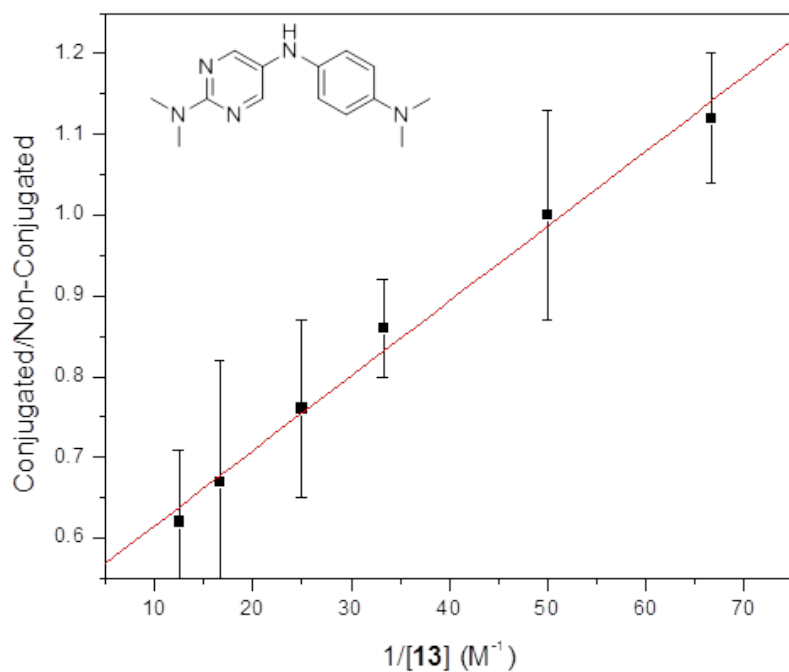
**Figure S4.** Double reciprocal plot used to obtain  $k_1 = 9.4 \times 10^4 \text{ M}^{-1}\text{s}^{-1}$  for compound **9**. Measurement was made using a phenyl-based peroxyester to improve resolution of a co-eluting peak observed when using the naphthyl-peroxyester described above.<sup>2</sup>



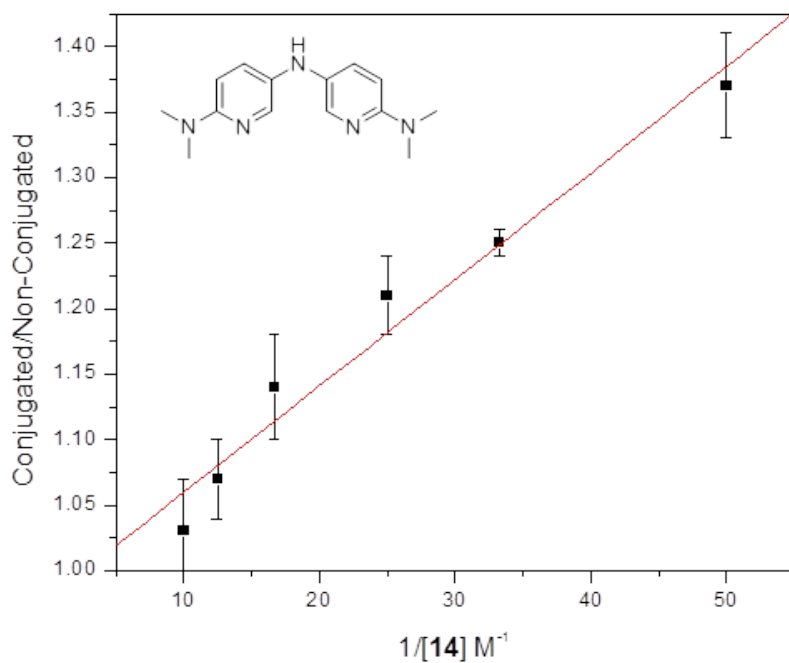
**Figure S5.** Double reciprocal plot used to obtain  $k_1 = 7.7 \times 10^4 \text{ M}^{-1}\text{s}^{-1}$  for compound **10**.



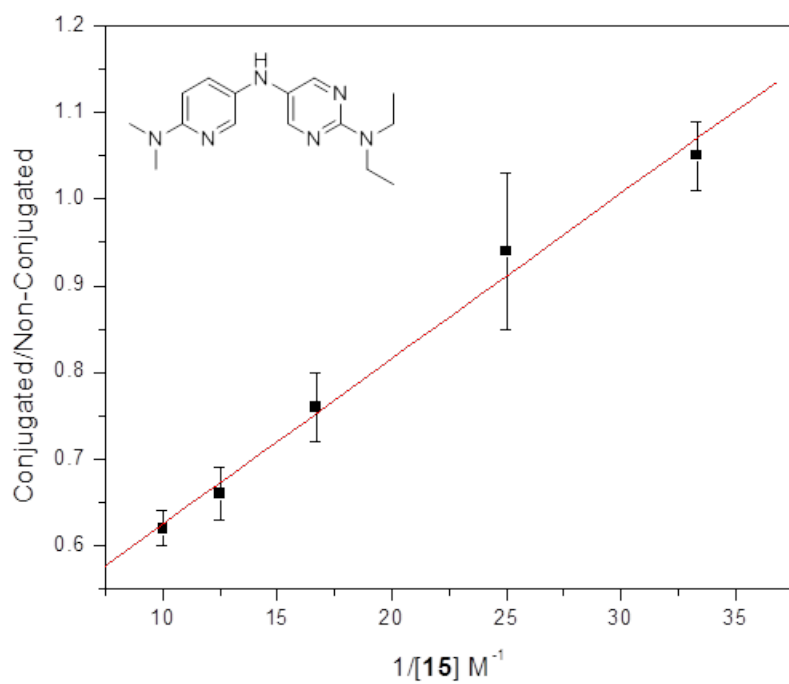
**Figure S6.** Double reciprocal plot used to obtain  $k_1 = 2.4 \times 10^4 \text{ M}^{-1}\text{s}^{-1}$  for compound **11**.



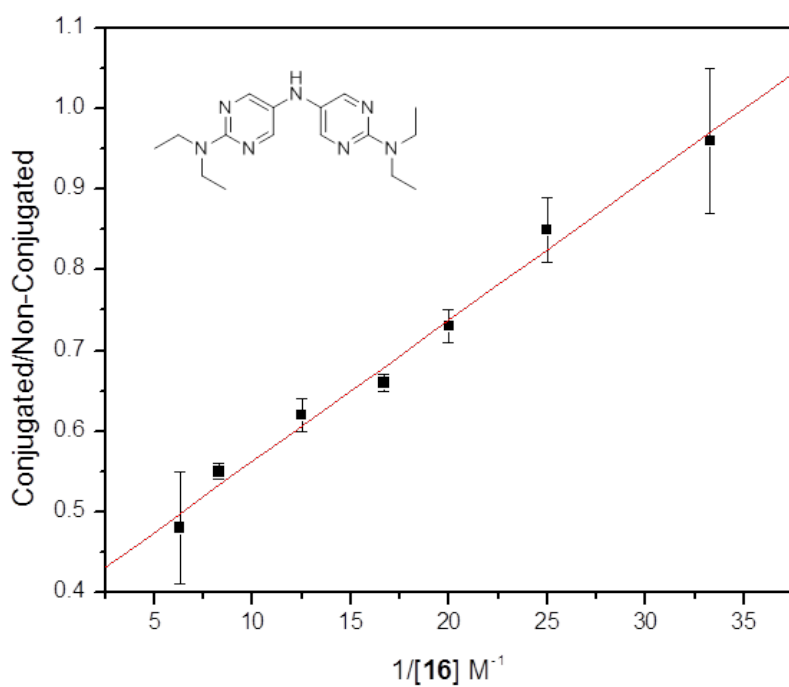
**Figure S7.** Double reciprocal plot used to obtain  $k_1 = 3.7 \times 10^7 \text{ M}^{-1}\text{s}^{-1}$  for compound **13**.



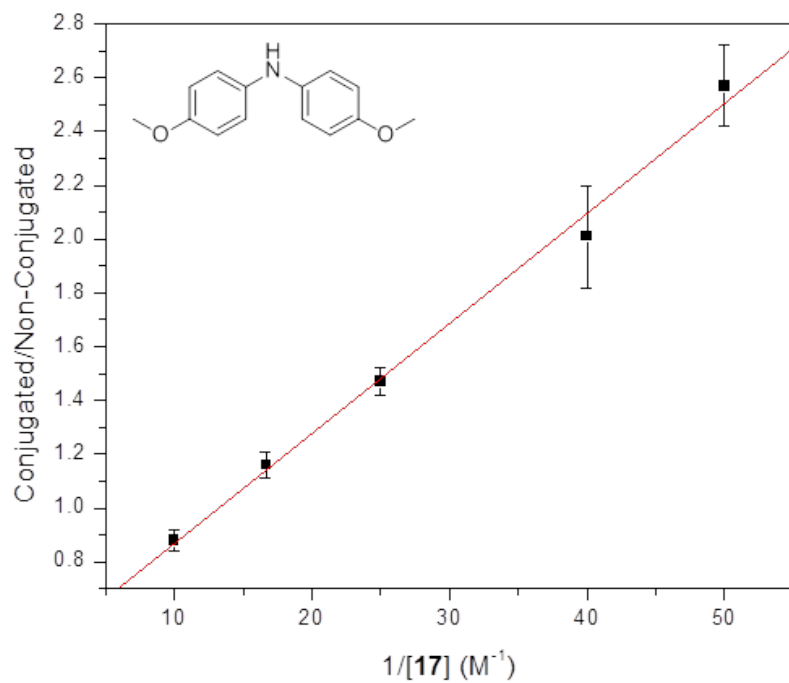
**Figure S8.** Double reciprocal plot used to obtain  $k_1 = 3.4 \times 10^7 \text{ M}^{-1}\text{s}^{-1}$  for compound **14**.



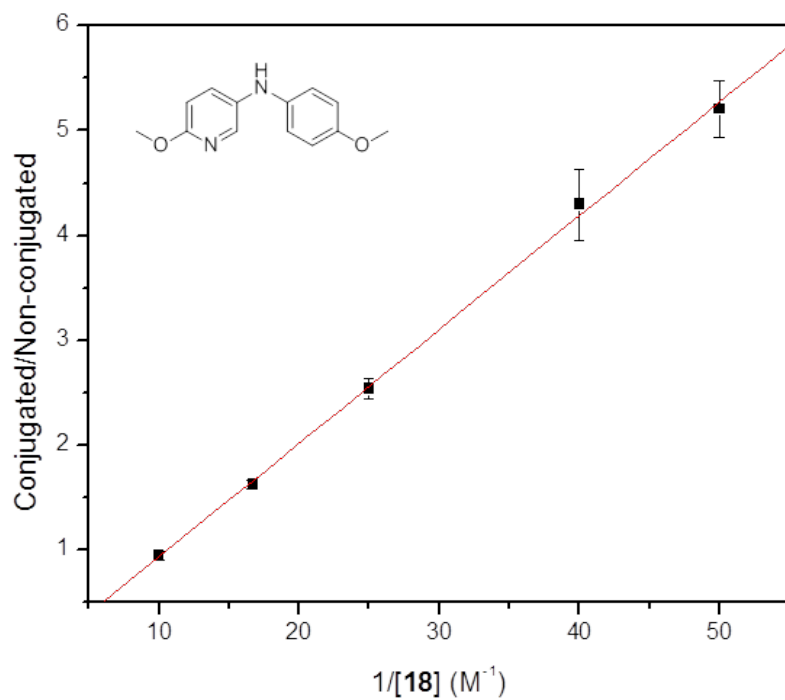
**Figure S9.** Double reciprocal plot used to obtain  $k_1 = 3.1 \times 10^7 \text{ M}^{-1}\text{s}^{-1}$  for compound **15**.



**Figure S10.** Double reciprocal plot used to obtain  $k_1 = 1.8 \times 10^7 \text{ M}^{-1}\text{s}^{-1}$  for compound **16**.

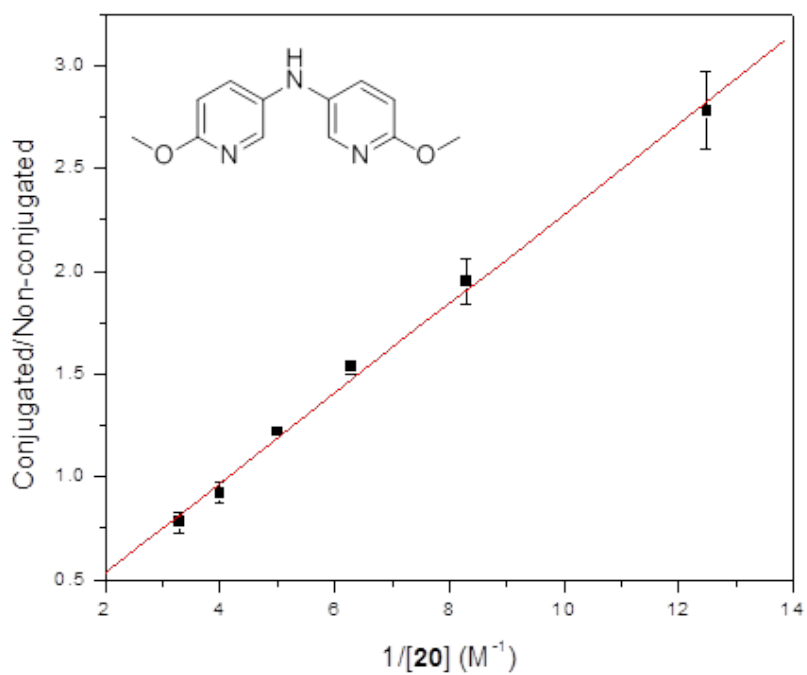


**Figure S11.** Double reciprocal plot used to obtain  $k_1 = 3.7 \times 10^6 \text{ M}^{-1}\text{s}^{-1}$  for compound **17**.

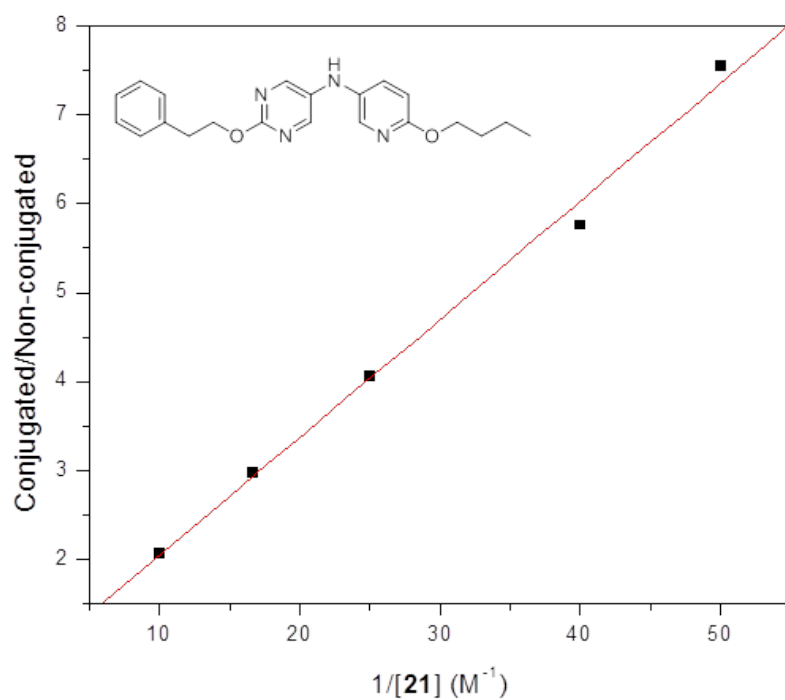


**Figure S12.** Double reciprocal plot used to obtain  $k_1 = 1.4 \times 10^6 \text{ M}^{-1}\text{s}^{-1}$  for compound **18**.

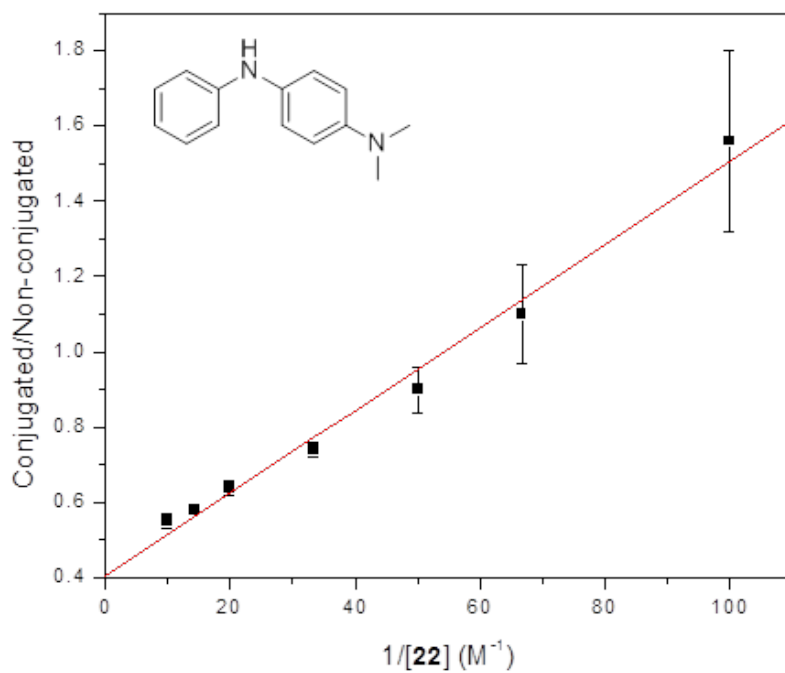




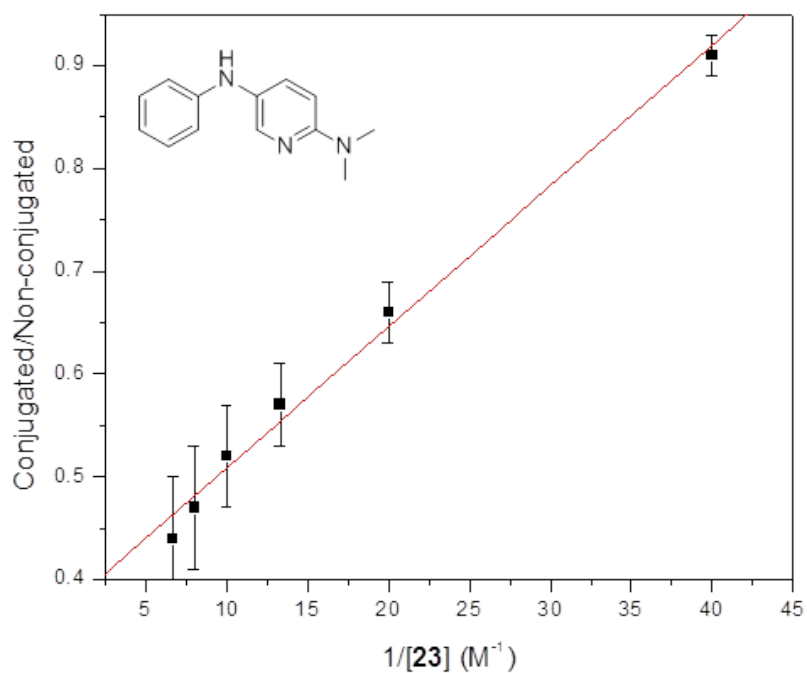
**Figure S13.** Double reciprocal plot used to obtain  $k_1 = 9.0 \times 10^5 \text{ M}^{-1}\text{s}^{-1}$  for compound **20**.



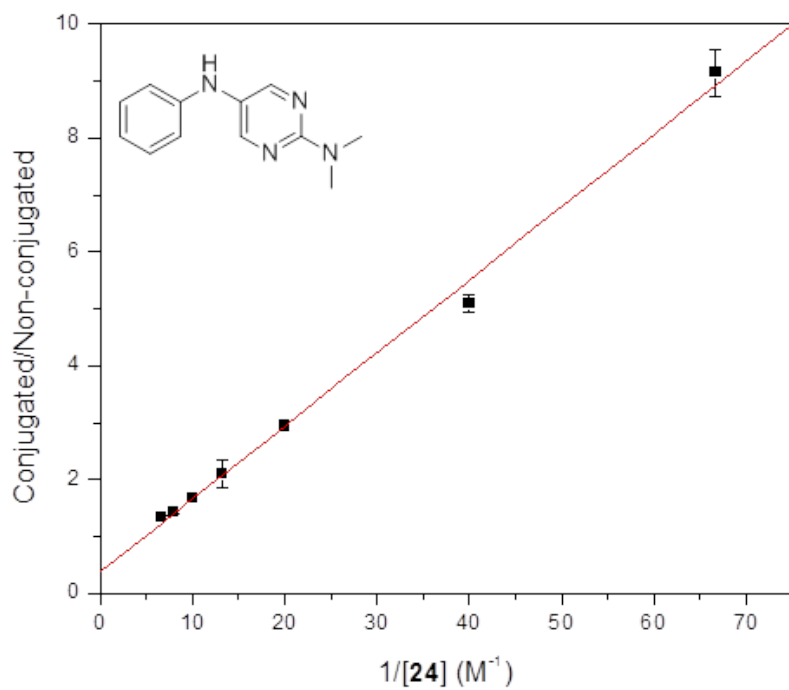
**Figure S14.** Double reciprocal plot used to obtain  $k_1 = 6.0 \times 10^5 \text{ M}^{-1}\text{s}^{-1}$  for compound **21**.



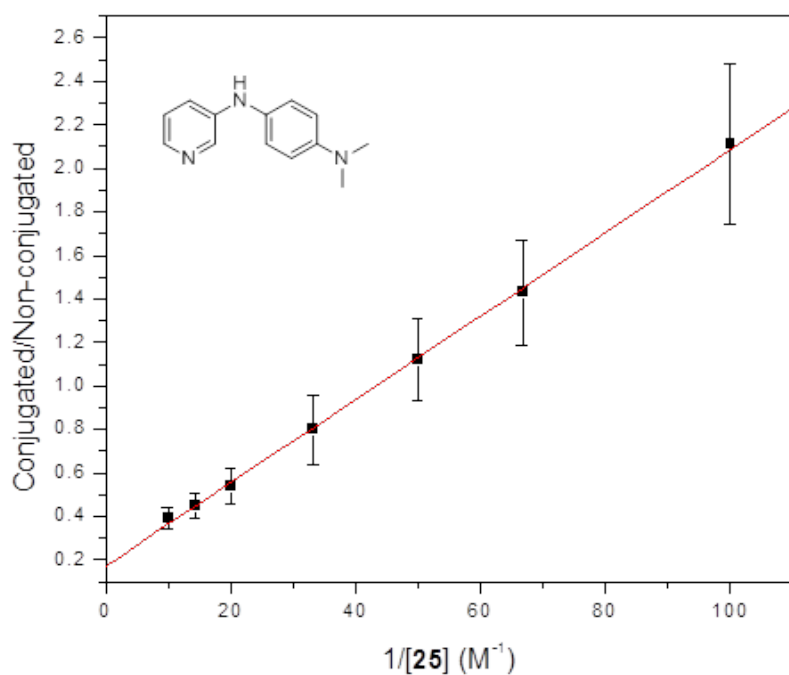
**Figure S15.** Double reciprocal plot used to obtain  $k_1 = 1.3 \times 10^7 \text{ M}^{-1}\text{s}^{-1}$  for compound **22**.



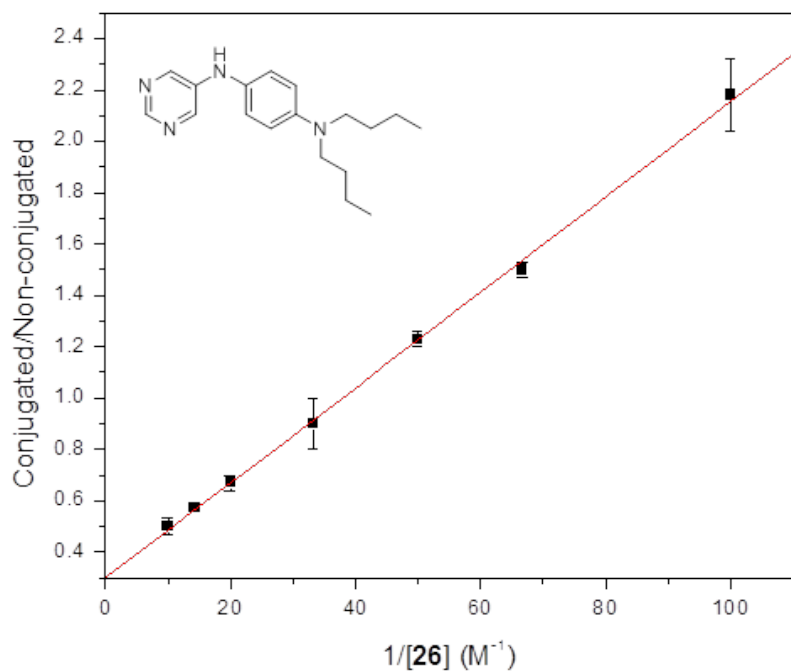
**Figure S16.** Double reciprocal plot used to obtain  $k_1 = 1.1 \times 10^7 \text{ M}^{-1}\text{s}^{-1}$  for compound **23**.



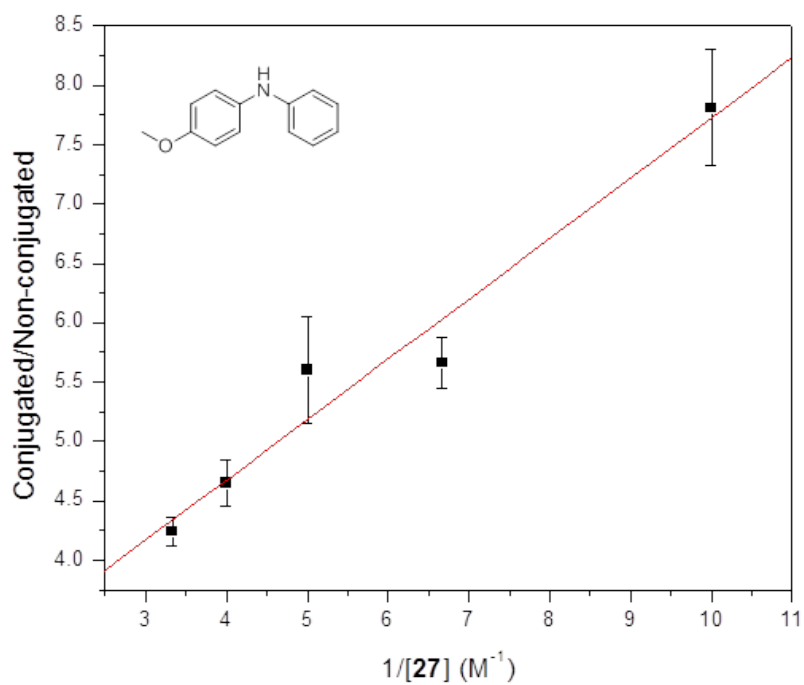
**Figure S17.** Double reciprocal plot used to obtain  $k_1 = 3.0 \times 10^6 \text{ M}^{-1}\text{s}^{-1}$  for compound **24**.



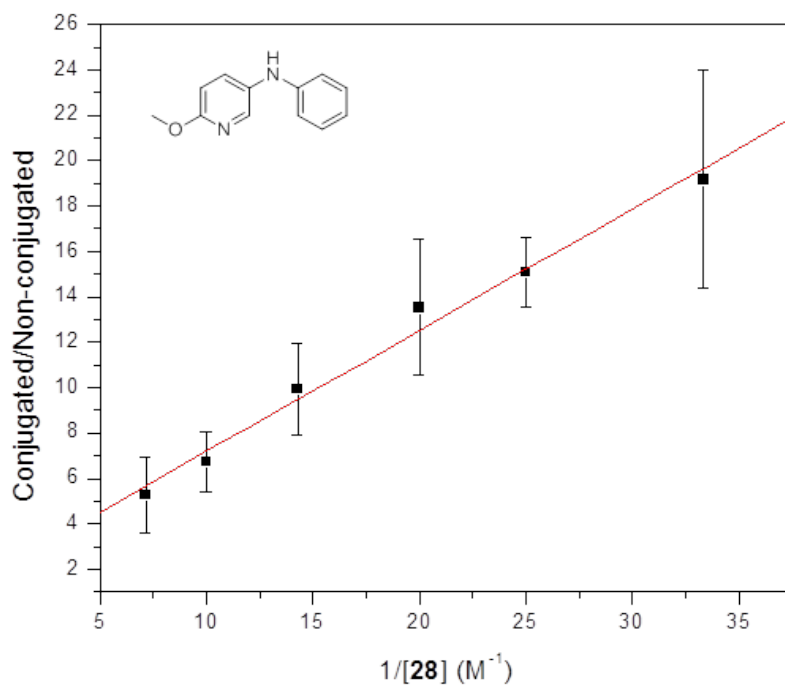
**Figure S18.** Double reciprocal plot used to obtain  $k_1 = 8.0 \times 10^6 \text{ M}^{-1}\text{s}^{-1}$  for compound **25**.



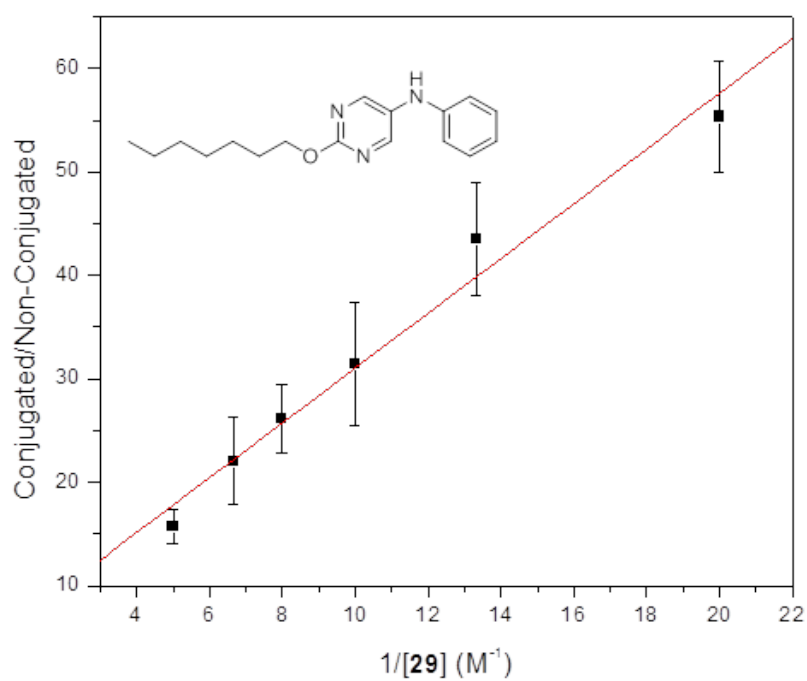
**Figure S19.** Double reciprocal plot used to obtain  $k_1 = 8.0 \times 10^6 \text{ M}^{-1}\text{s}^{-1}$  for compound **26**.



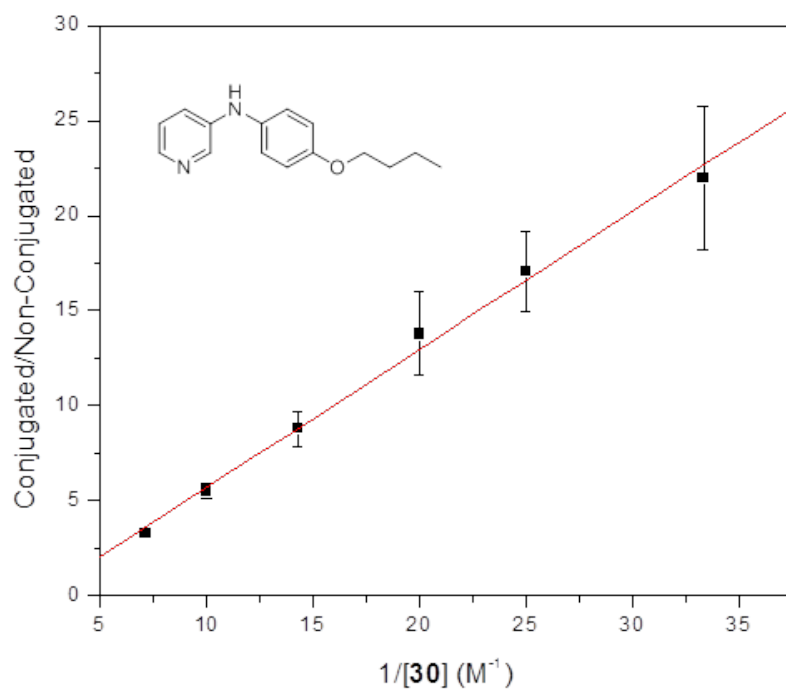
**Figure S20.** Double reciprocal plot used to obtain  $k_1 = 3.2 \times 10^5 \text{ M}^{-1}\text{s}^{-1}$  for compound **27**.



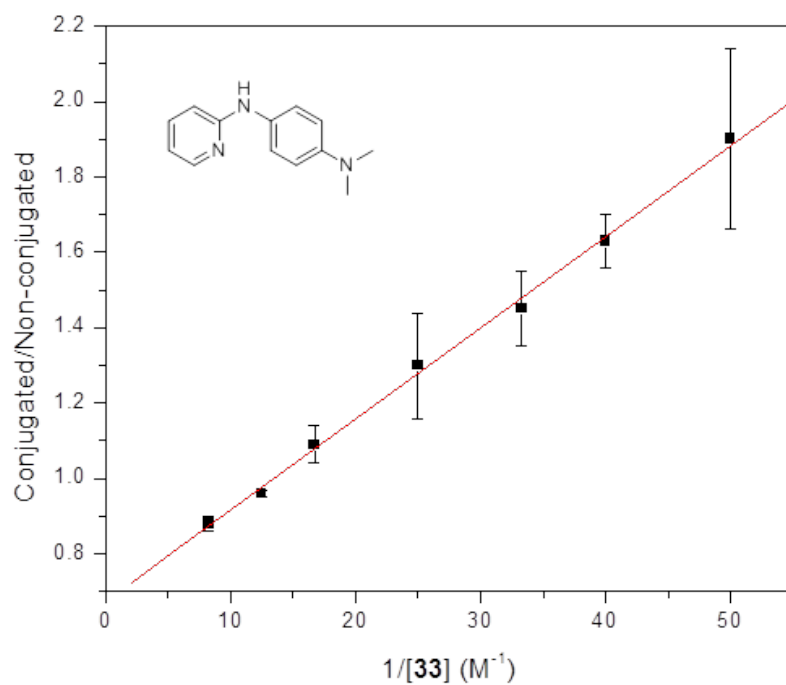
**Figure S21.** Double reciprocal plot used to obtain  $k_1 = 2.9 \times 10^5 \text{ M}^{-1}\text{s}^{-1}$  for compound **28**.



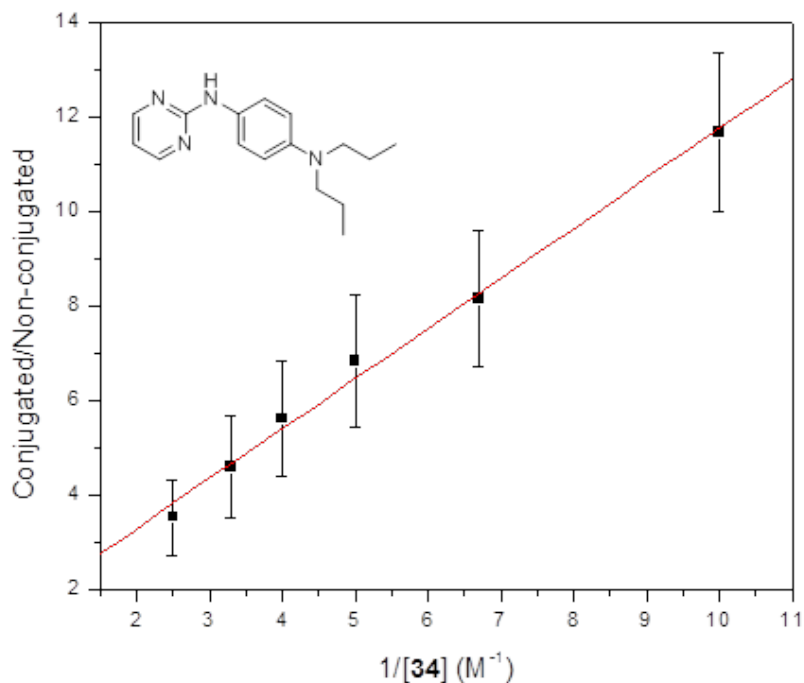
**Figure S22.** Double reciprocal plot used to obtain  $k_1 = 6.0 \times 10^4 \text{ M}^{-1}\text{s}^{-1}$  for compound **29**.



**Figure S23.** Double reciprocal plot used to obtain  $k_1 = 2.1 \times 10^5 M^{-1}s^{-1}$  for compound **30**.



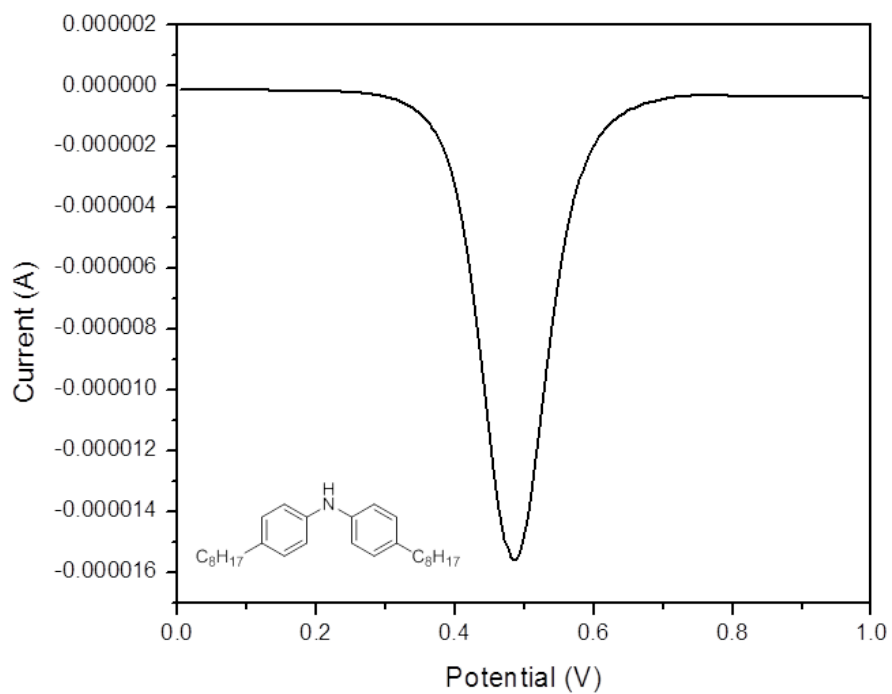
**Figure S24.** Double reciprocal plot used to obtain  $k_1 = 6.4 \times 10^6 M^{-1}s^{-1}$  for compound **33**.



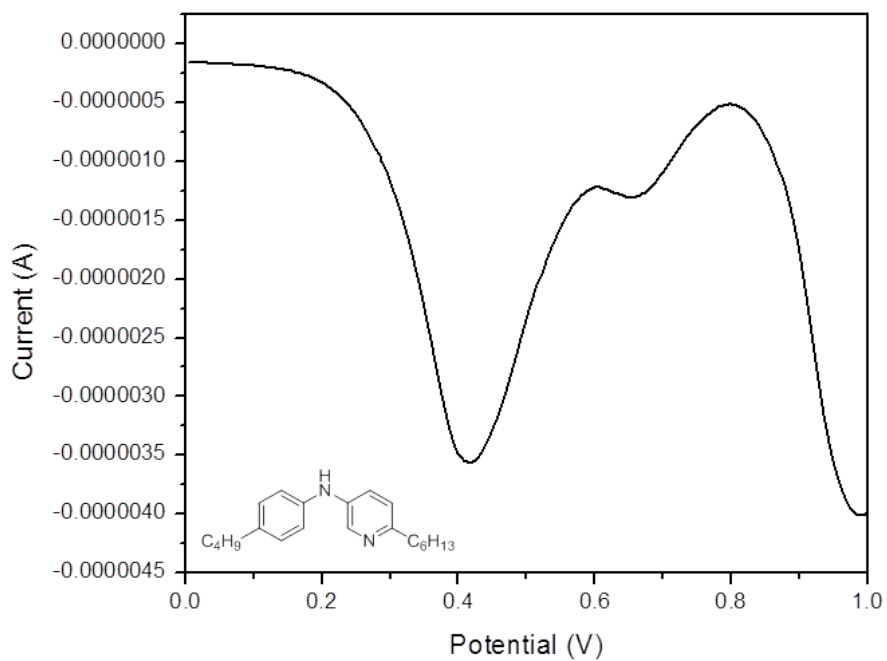
**Figure S25.** Double reciprocal plot used to obtain  $k_1 = 1.5 \times 10^5 \text{ M}^{-1}\text{s}^{-1}$  for compound **34**.

### Voltammetry Experiments

Standard potentials (CV) and anodic peak potentials (DPV) were measured using a BASi potentiostat with a glassy-carbon working electrode, a platinum counter electrode and an Ag/AgNO<sub>3</sub> (0.005 M) reference electrode. Samples were measured in dry acetonitrile using Bu<sub>4</sub>N•PF<sub>6</sub> (0.1 M) as an electrolyte at 25 °C. For compounds displaying reversible redox chemistry, cyclic voltammograms were obtained using a scan rate of 100 mV/s. For compounds with no reversible properties, differential pulse voltammograms were obtained using a scan rate of 20 mV/s.

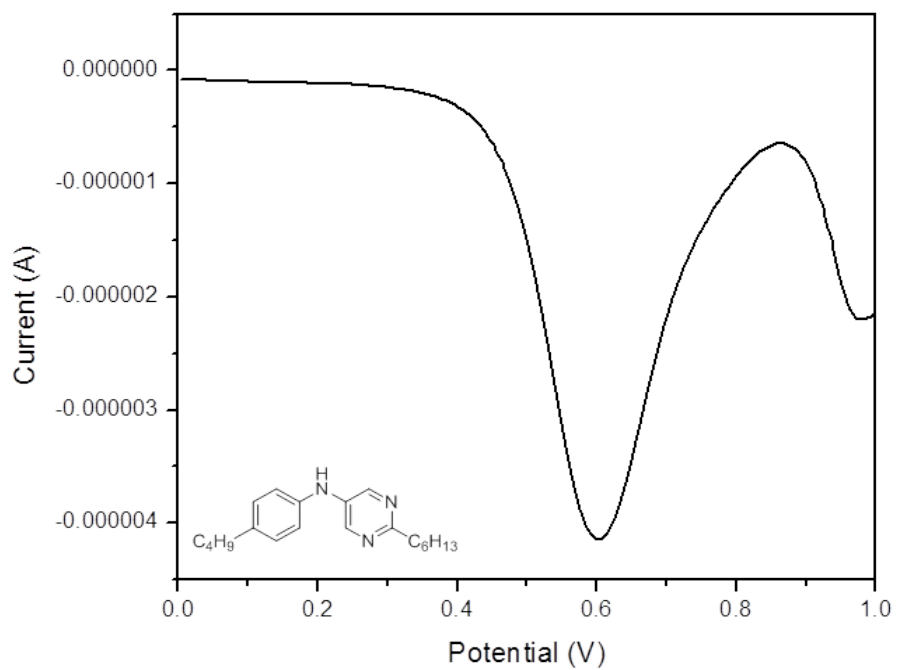


**Figure S25.** Differential pulse voltammogram of **2** vs.  $\text{Ag}/\text{Ag}^+$ .  $E_{\text{pa}} = 1.02$  V vs. NHE.

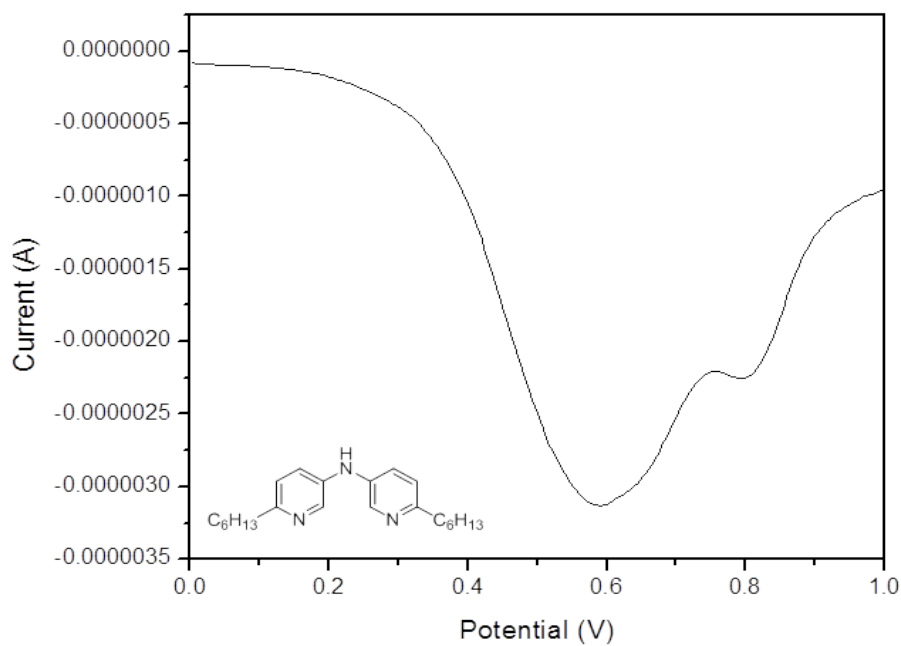


**Figure S26.** Differential pulse voltammogram of **7** vs.  $\text{Ag}/\text{Ag}^+$ .  $E_{\text{pa}} = 0.95$  V vs. NHE.

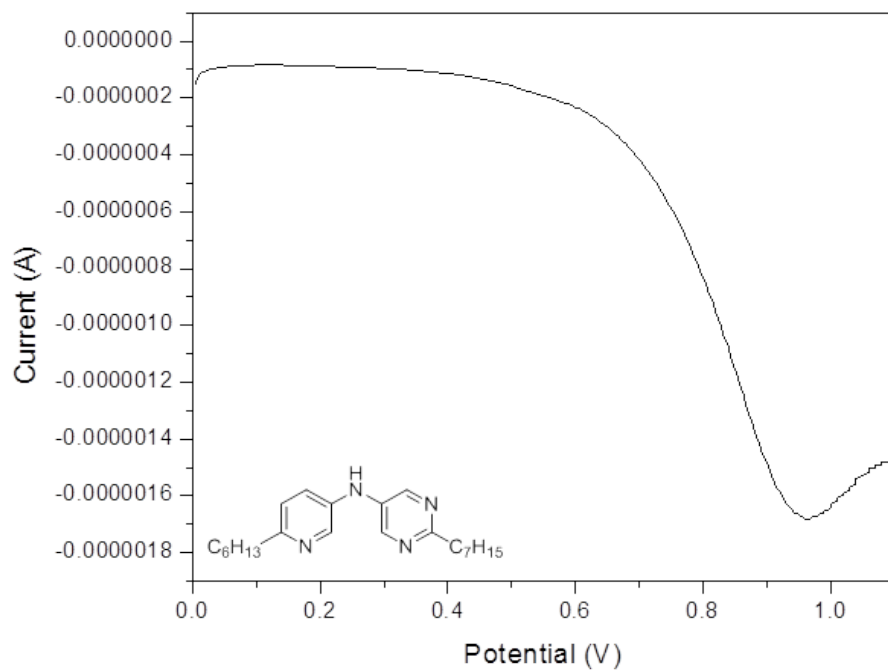




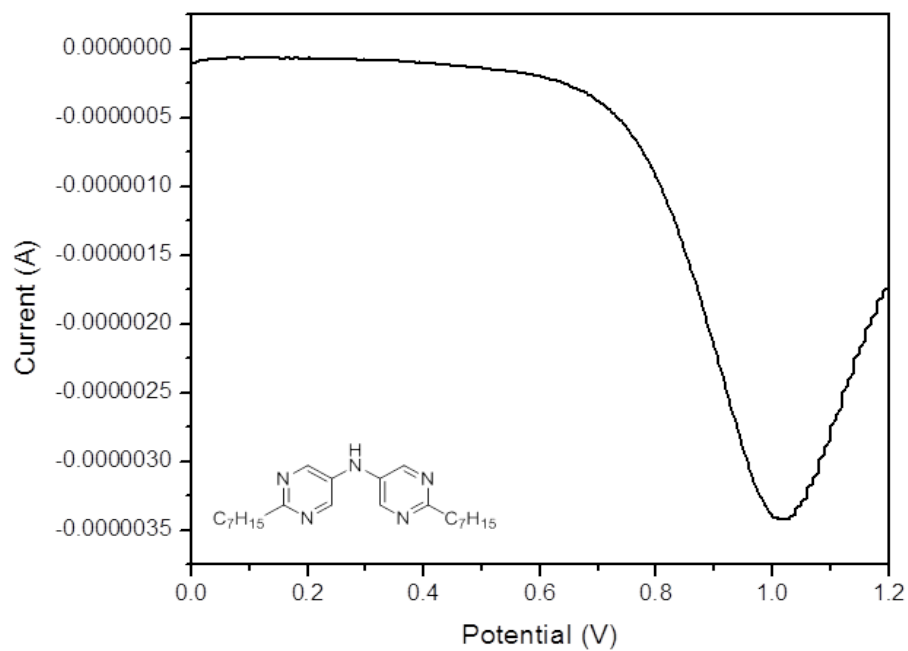
**Figure S27.** Differential pulse voltammogram of **8** vs.  $\text{Ag}/\text{Ag}^+$ .  $E_{\text{pa}} = 0.95$  V vs. NHE.



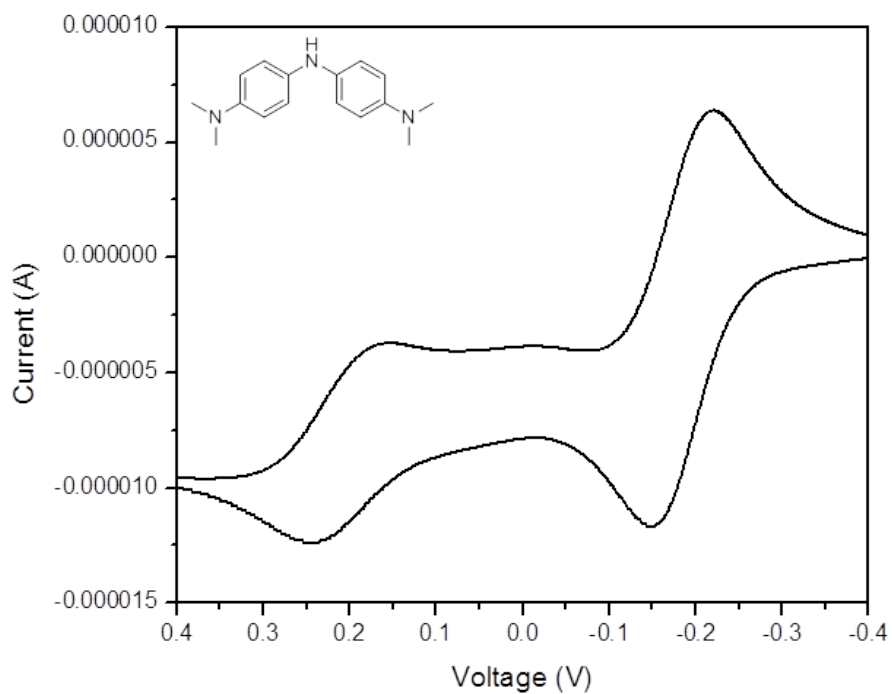
**Figure S28.** Differential pulse voltammogram of **9** vs.  $\text{Ag}/\text{Ag}^+$ .  $E_{\text{pa}} = 1.12$  V vs. NHE.



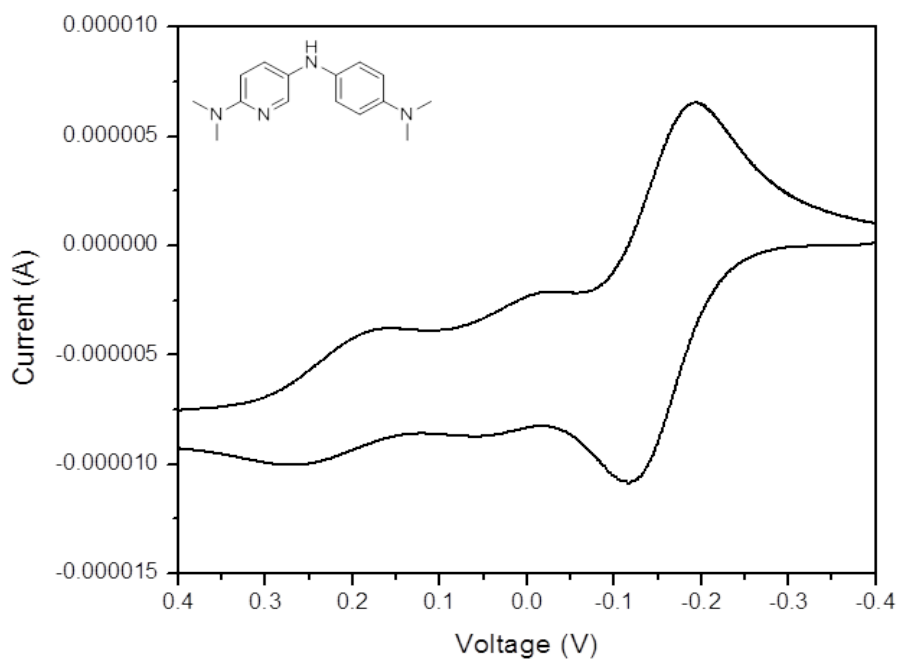
**Figure S29.** Differential pulse voltammogram of **10** vs. Ag/Ag<sup>+</sup>.  $E_{pa} = 1.50$  V vs. NHE.



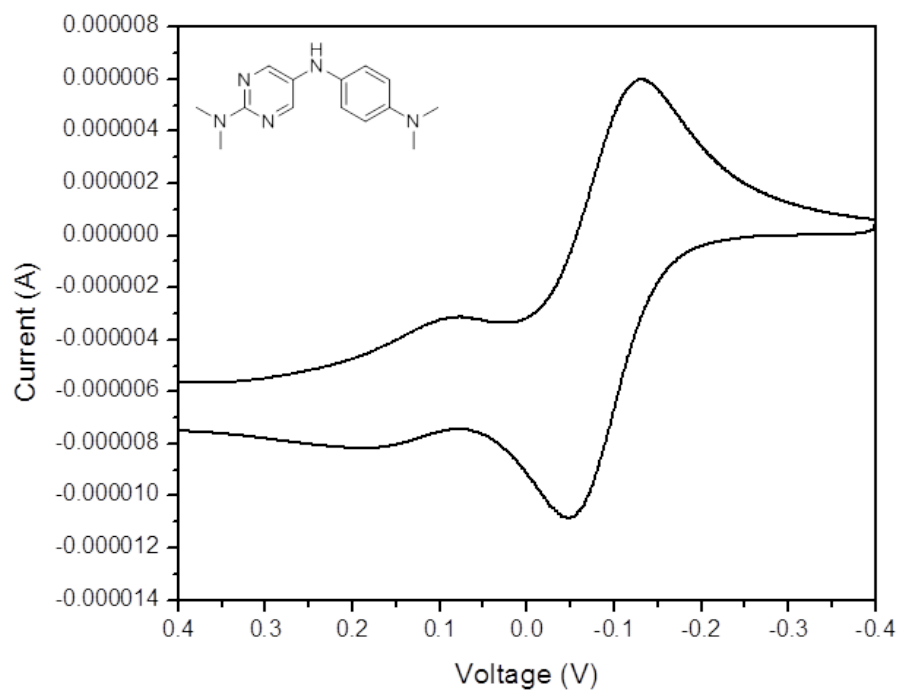
**Figure S30.** Differential pulse voltammogram of **11** vs. Ag/Ag<sup>+</sup>.  $E_{pa} = 1.55$  V vs. NHE.



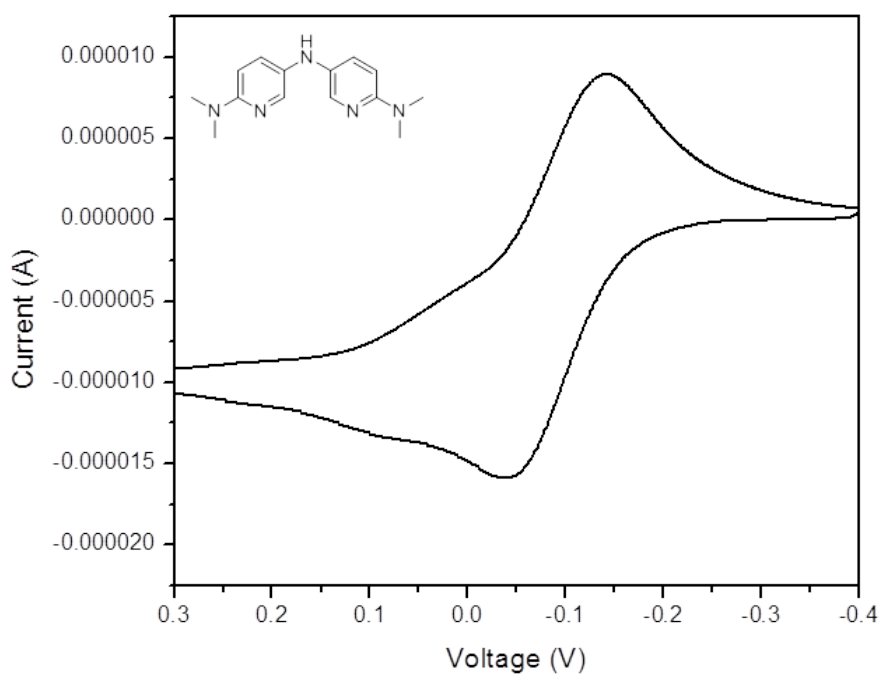
**Figure S31.** Cyclic voltammogram of **3** vs.  $\text{Ag}/\text{Ag}^+$ .  $E^\circ = 0.34 \text{ V}$  vs. NHE.



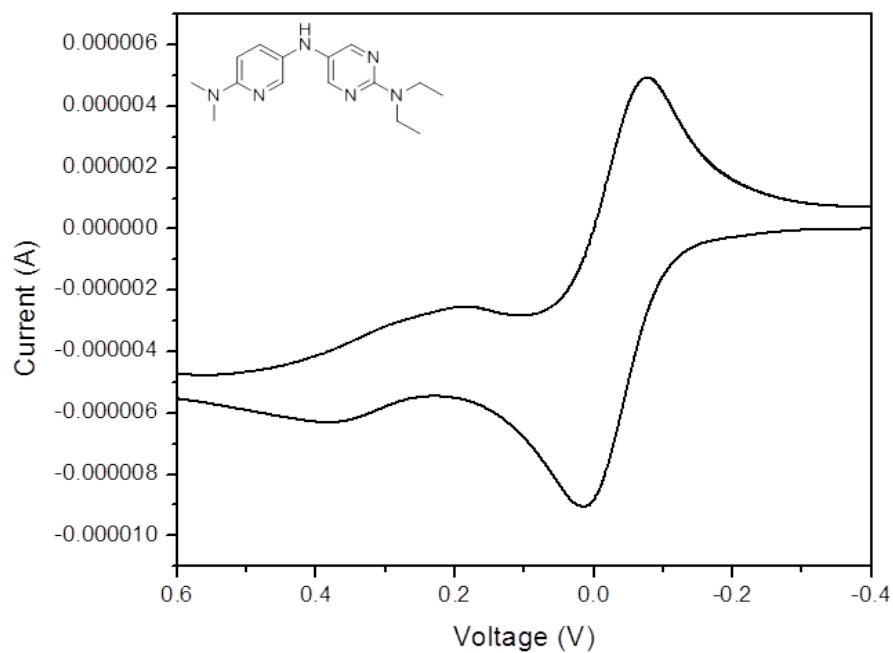
**Figure S32.** Cyclic voltammogram of **12** vs.  $\text{Ag}/\text{Ag}^+$ .  $E^\circ = 0.37 \text{ V}$  vs. NHE.



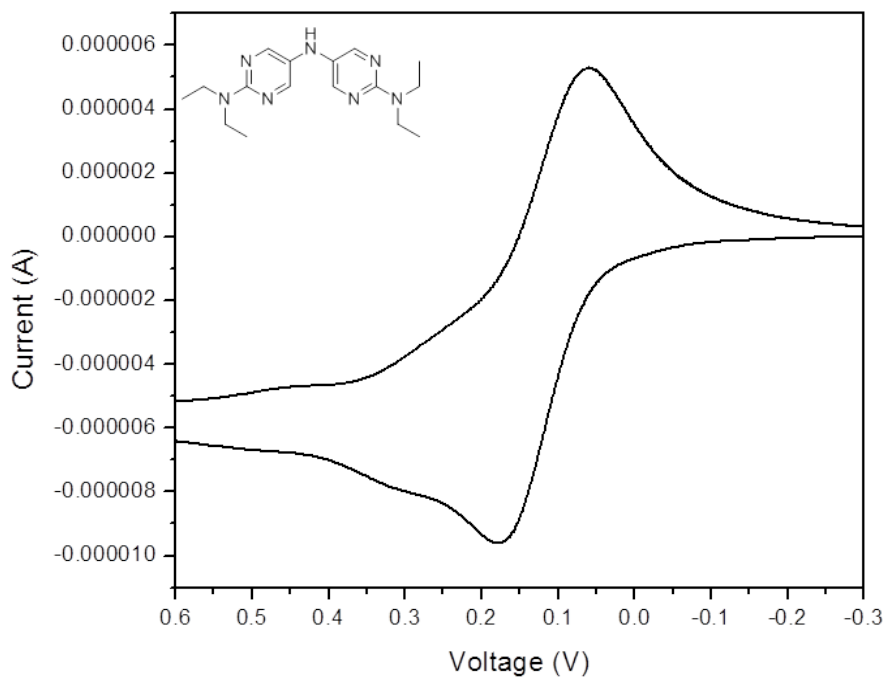
**Figure S33.** Cyclic voltammogram of **13** vs.  $\text{Ag}/\text{Ag}^+$ .  $E^\circ = 0.44$  V vs. NHE.



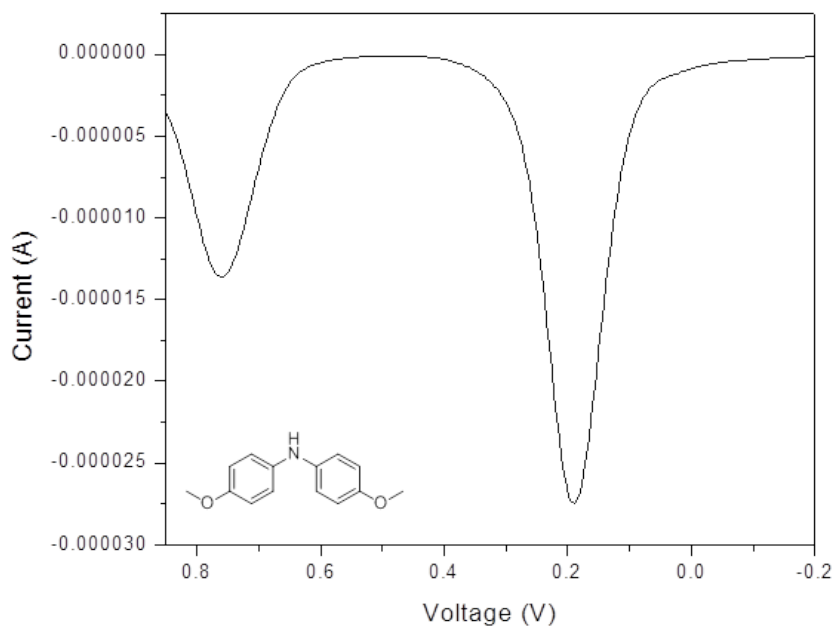
**Figure S34.** Cyclic voltammogram of **14** vs.  $\text{Ag}/\text{Ag}^+$ .  $E^\circ = 0.44$  V vs. NHE.



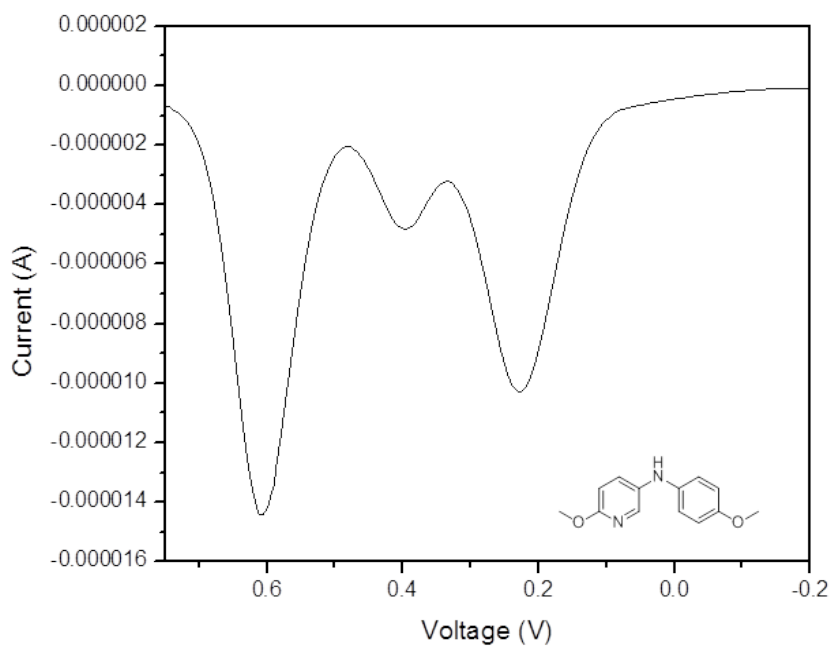
**Figure S35.** Cyclic voltammogram of **15** vs.  $\text{Ag}/\text{Ag}^+$ .  $E^\circ = 0.50$  V vs. NHE.



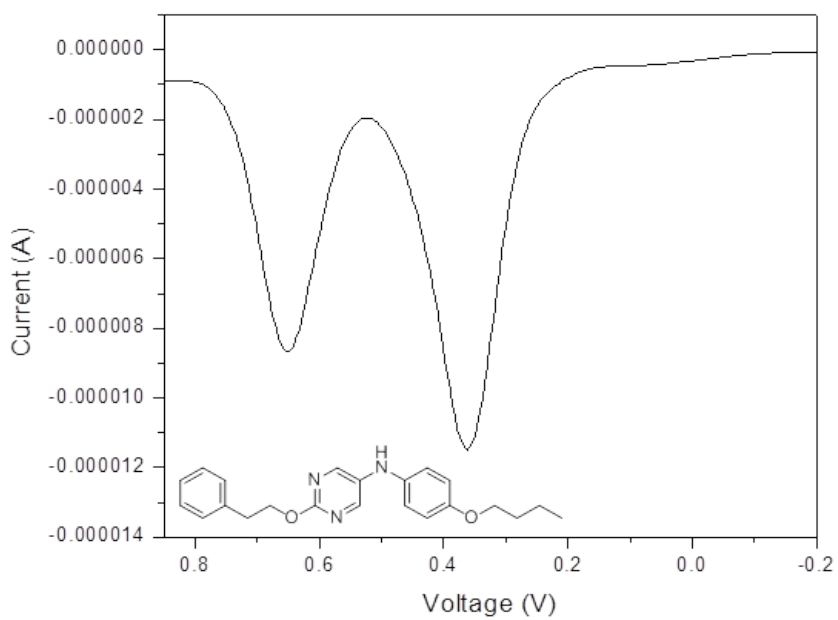
**Figure S36.** Cyclic voltammogram of **16** vs.  $\text{Ag}/\text{Ag}^+$ .  $E^\circ = 0.65$  V vs. NHE.



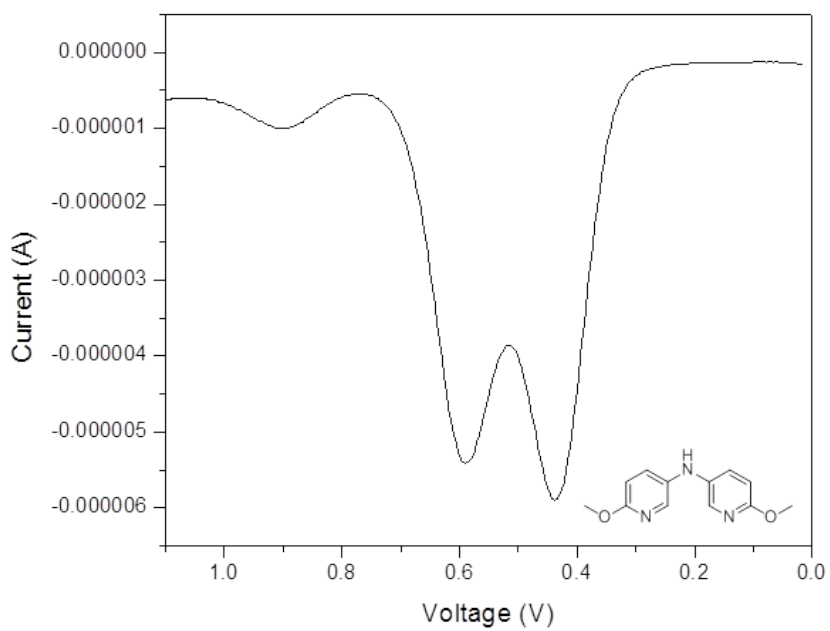
**Figure S36.** Cyclic voltammogram of **17** vs.  $\text{Ag}/\text{Ag}^+$ .  $E_{\text{pa}} = 0.70$  V vs. NHE.



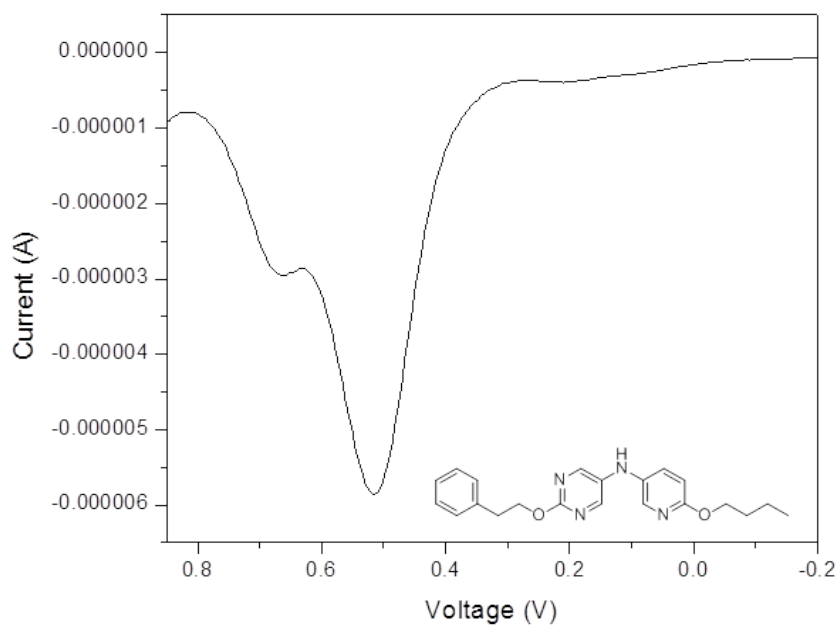
**Figure S37.** Cyclic voltammogram of **18** vs.  $\text{Ag}/\text{Ag}^+$ .  $E_{\text{pa}} = 0.74$  V vs. NHE.



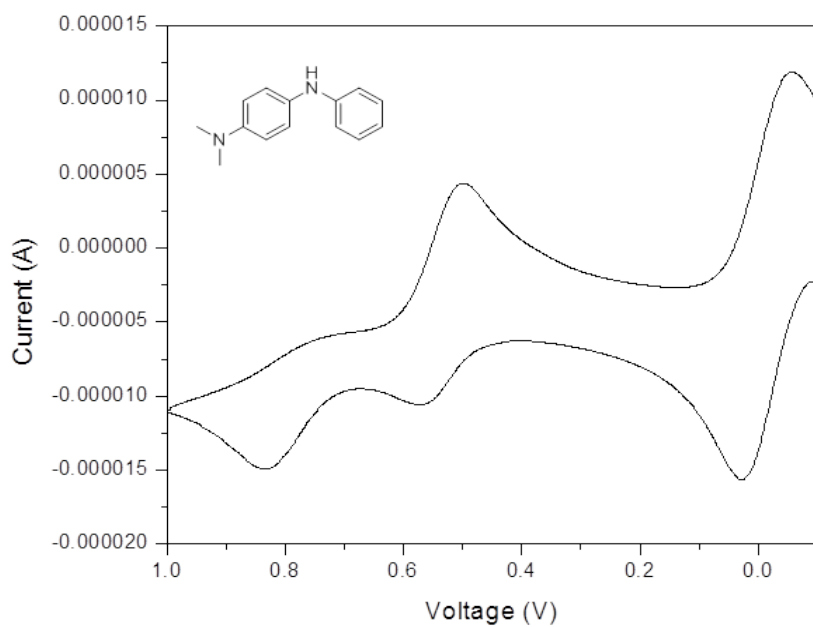
**Figure S38.** Cyclic voltammogram of **19** vs.  $\text{Ag}/\text{Ag}^+$ .  $E_{\text{pa}} = 0.88$  V vs. NHE.



**Figure S39.** Cyclic voltammogram of **20** vs.  $\text{Ag}/\text{Ag}^+$ .  $E_{\text{pa}} = 0.95$  V vs. NHE.

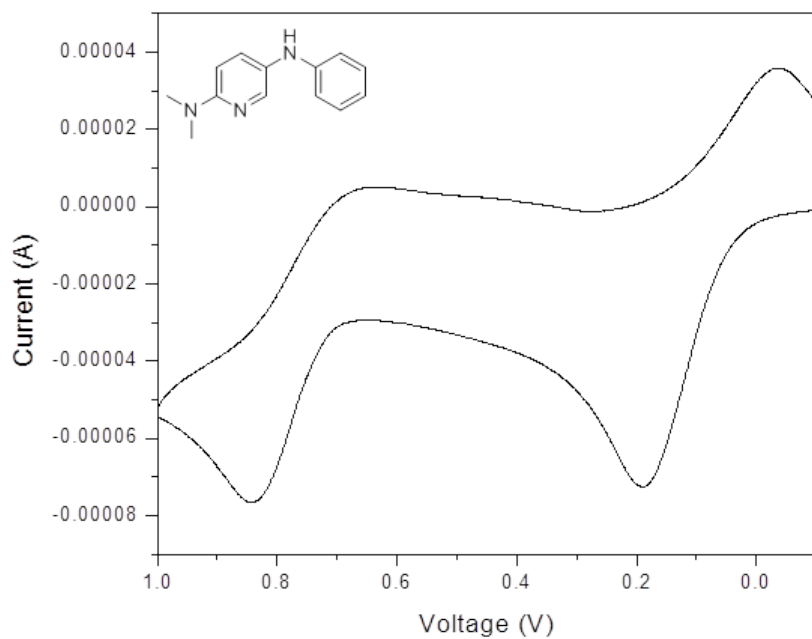


**Figure S40.** Cyclic voltammogram of **21** vs.  $\text{Ag}/\text{Ag}^+$ .  $E_{\text{pa}} = 1.03$  V vs. NHE.

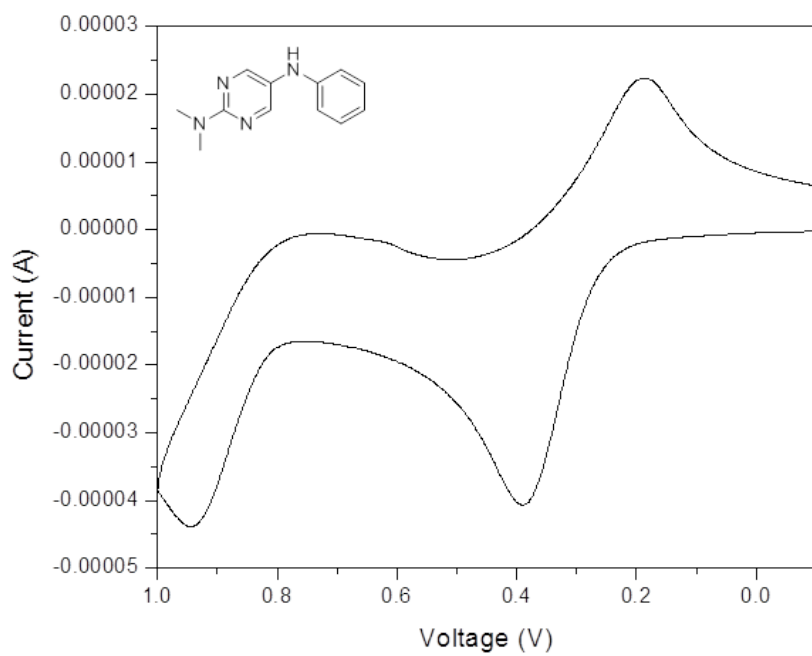


**Figure S41.** Cyclic voltammogram of **22** vs.  $\text{Ag}/\text{Ag}^+$ .  $E^\circ = 0.51$  V vs. NHE.

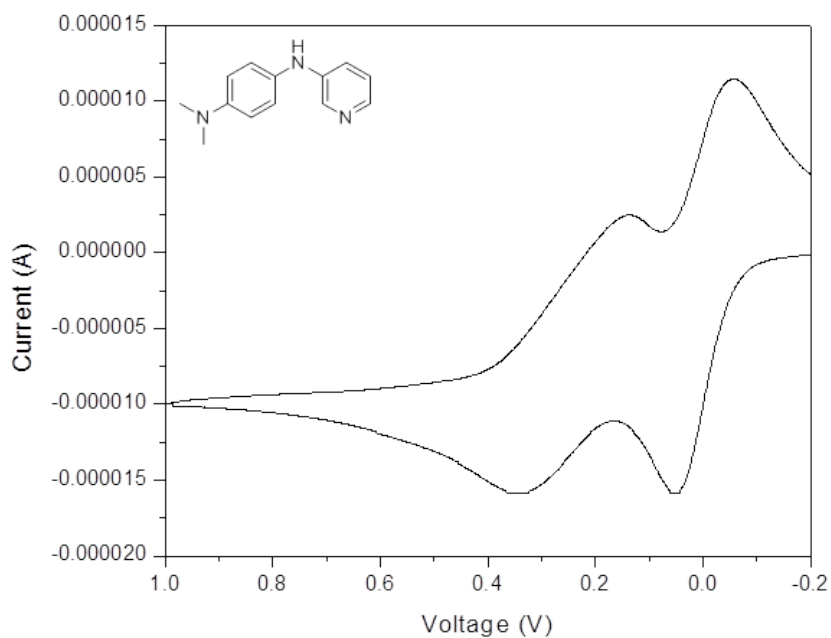




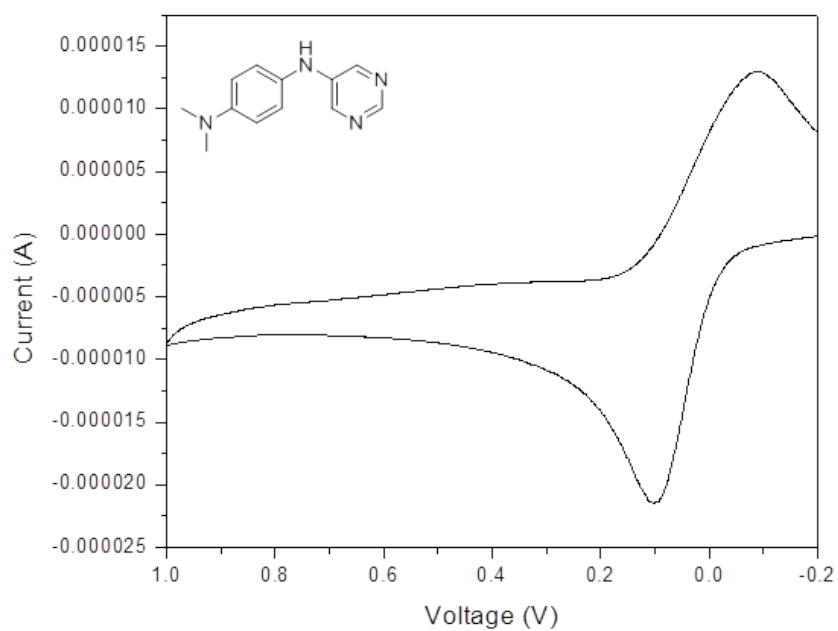
**Figure S42.** Cyclic voltammogram of **23** vs.  $\text{Ag}/\text{Ag}^+$ .  $E^\circ = 0.60$  V vs. NHE.



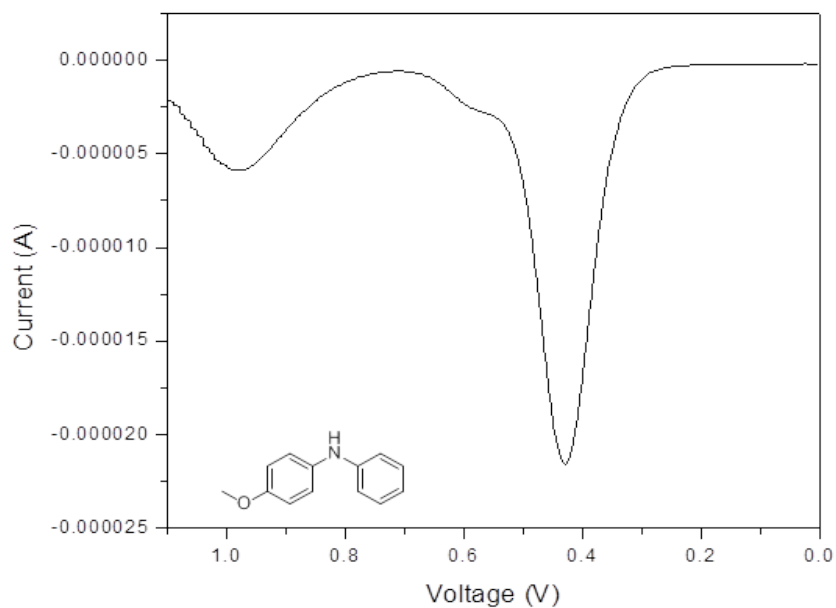
**Figure S43.** Cyclic voltammogram of **24** vs.  $\text{Ag}/\text{Ag}^+$ .  $E^\circ = 0.81$  V vs. NHE.



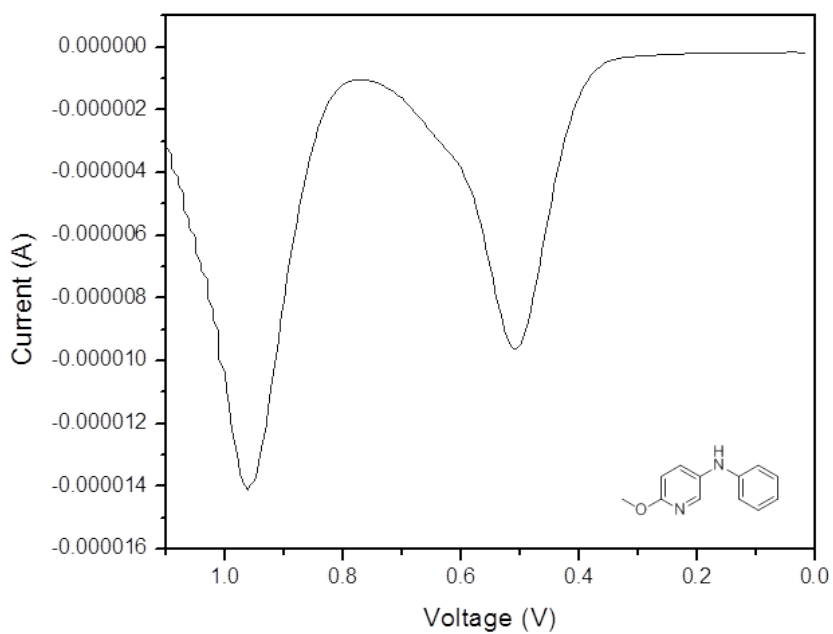
**Figure S44.** Cyclic voltammogram of **25** vs.  $\text{Ag}/\text{Ag}^+$ .  $E^\circ = 0.53$  V vs. NHE.



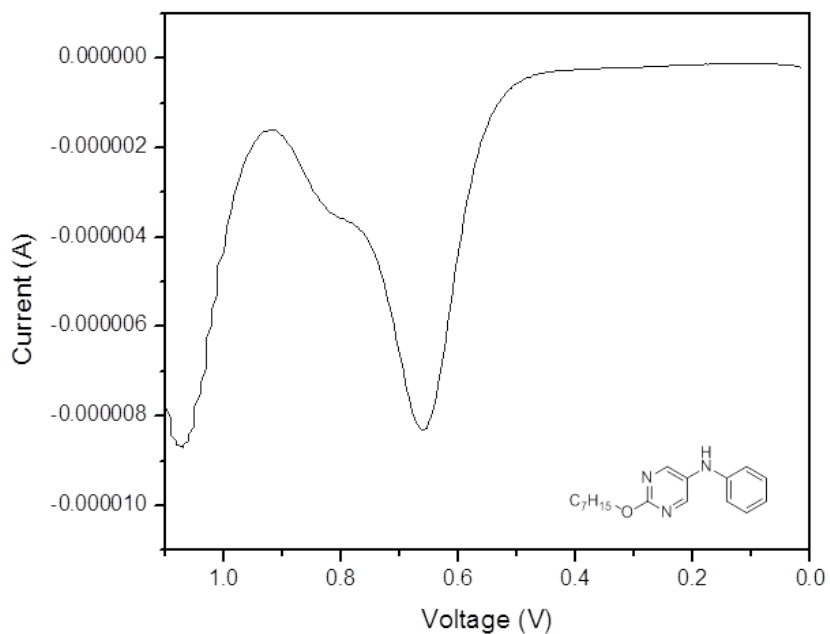
**Figure S45.** Cyclic voltammogram of **26** vs.  $\text{Ag}/\text{Ag}^+$ .  $E^\circ = 0.56$  V vs. NHE.



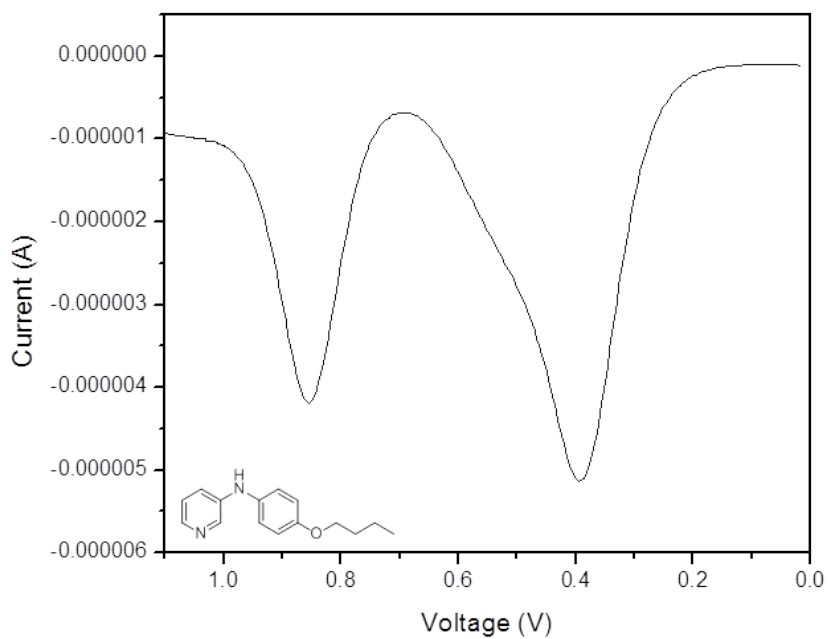
**Figure S46.** Cyclic voltammogram of **27** vs.  $\text{Ag}/\text{Ag}^+$ .  $E_{\text{pa}} = 0.94$  V vs. NHE.



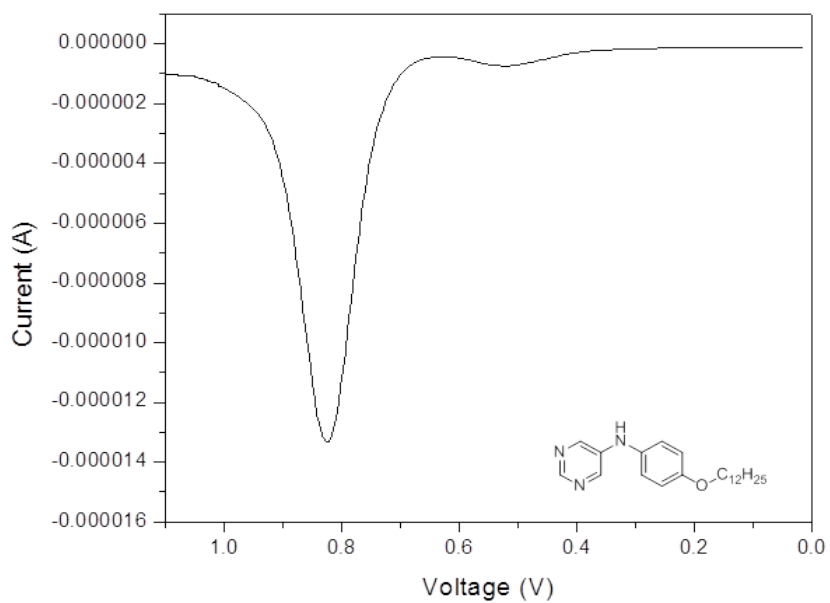
**Figure S47.** Cyclic voltammogram of **28** vs.  $\text{Ag}/\text{Ag}^+$ .  $E_{\text{pa}} = 1.02$  V vs. NHE.



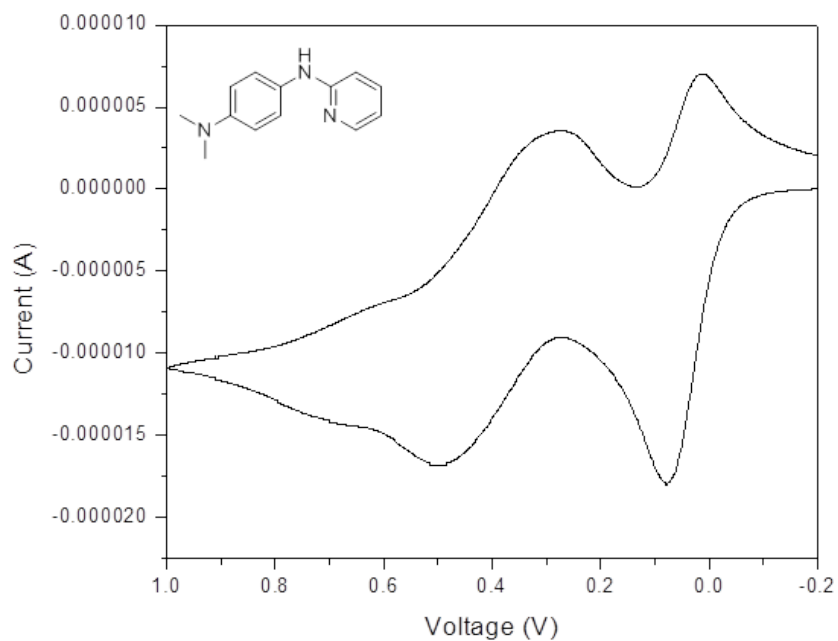
**Figure S48.** Cyclic voltammogram of **29** vs.  $\text{Ag}/\text{Ag}^+$ .  $E_{\text{pa}} = 1.17$  V vs. NHE.



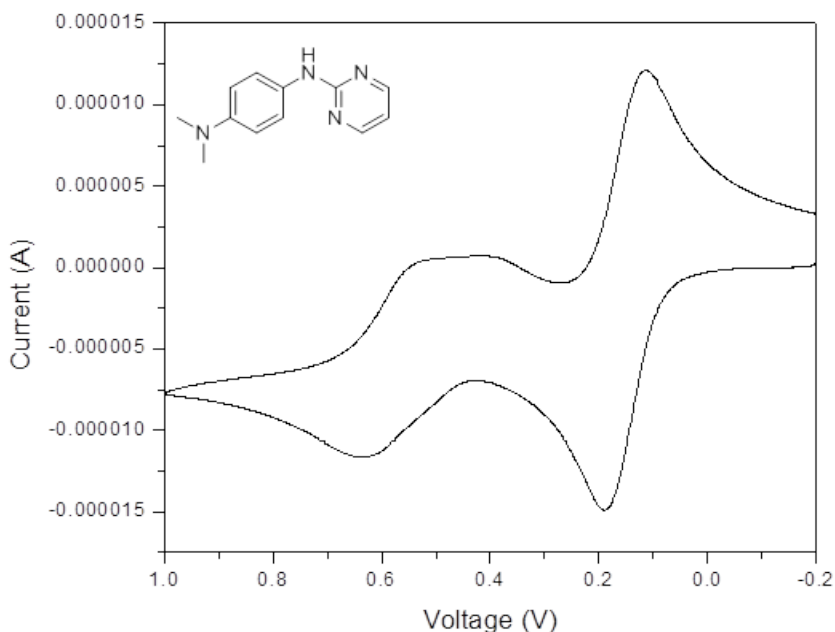
**Figure S49.** Cyclic voltammogram of **30** vs.  $\text{Ag}/\text{Ag}^+$ .  $E_{\text{pa}} = 0.90$  V vs. NHE.



**Figure S50.** Cyclic voltammogram of **31** vs.  $\text{Ag}/\text{Ag}^+$ .  $E_{\text{pa}} = 1.34$  V vs. NHE.



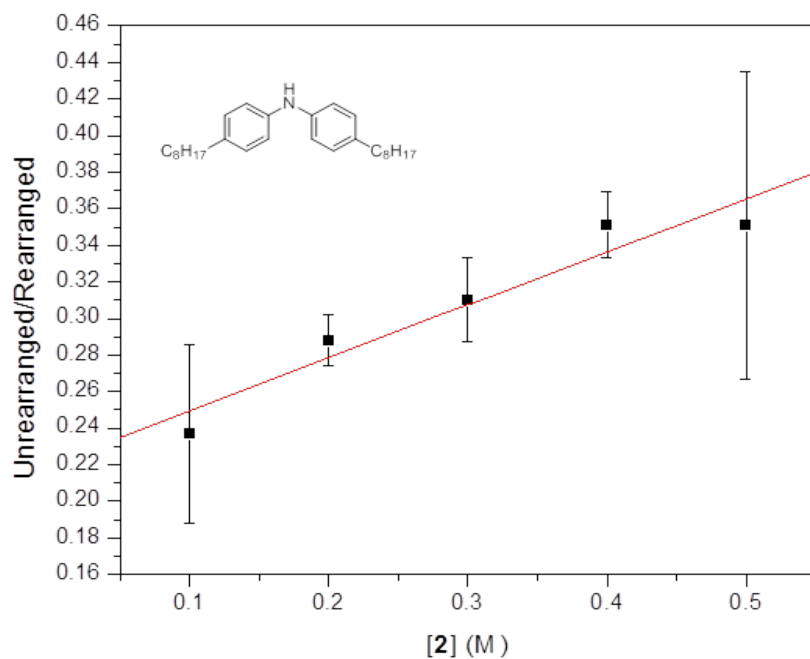
**Figure S51.** Cyclic voltammogram of **33** vs.  $\text{Ag}/\text{Ag}^+$ .  $E_{\text{pa}} = 0.57$  V vs. NHE.



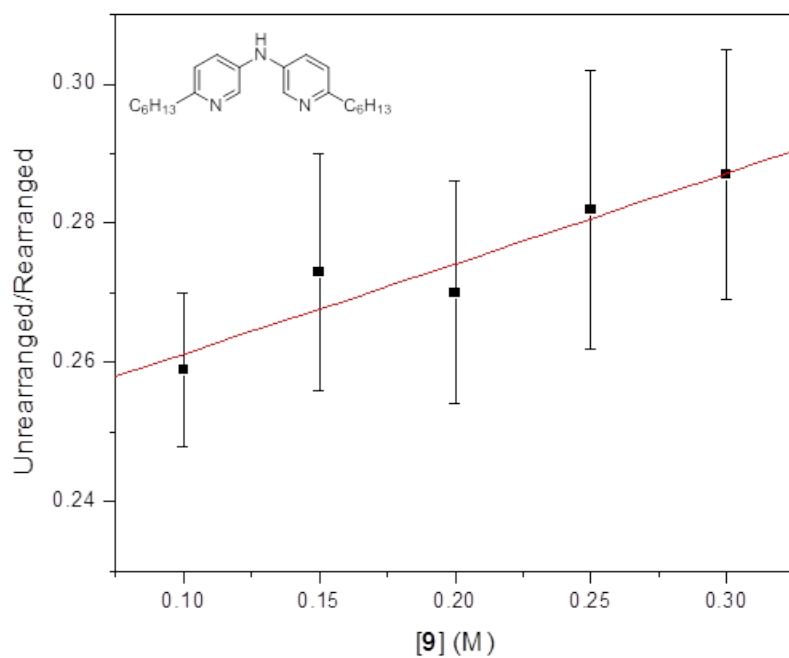
**Figure S52.** Cyclic voltammogram of **34** vs.  $\text{Ag}/\text{Ag}^+$ .  $E_{\text{pa}} = 0.64$  V vs. NHE.

### Alkyl Radical Kinetics

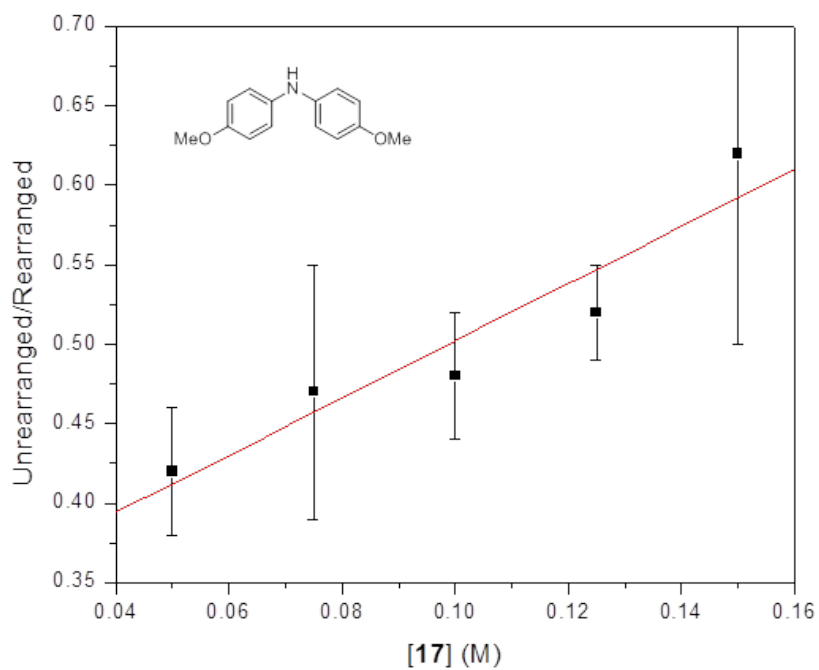
Rate constants for trapping alkyl radicals were obtained by alkyl radical clock techniques. A 100  $\mu\text{L}$  sample containing diarylamine (0.02-0.25 M, depending on  $k_{\text{H}}$ ), bis(triphenylstannane) (0.01 M) and 2-(2-bromo-1,1-dimethylethyl)-naphthalene<sup>3</sup> (0.01 M) in chlorobenzene was degassed by sparging with argon for 2 minutes. The sample was then irradiated for 20 minutes in a Luzchem photoreactor equipped with UVC germicidal lamps (strong line at 254 nm). The samples were transferred to GC vials and diluted with acetonitrile (300  $\mu\text{L}$ ) for analysis. GC analysis was carried out using an Agilent DB-5 column (30 m x 0.32  $\mu\text{m}$  x 0.25  $\mu\text{m}$ ) with the following temperature profile: 70  $^{\circ}\text{C}$  hold 0.5 min, 1  $^{\circ}\text{C}/\text{min}$  to 82  $^{\circ}\text{C}$ , 20  $^{\circ}\text{C}/\text{min}$  to 280  $^{\circ}\text{C}$ , hold 5 min. A plot of Unrearranged/rearranged products was plotted vs.  $[\text{Ar}_2\text{NH}]$  to obtain  $k_{\text{H}}$  values ( $k_{\text{r}} = 1.4 \times 10^4 \text{ s}^{-1}$ ). Preparation of GC standards: 2-*tert*-butylnaphthalene and 2-*iso*-butyl-naphthalene were prepared by treating 2-(2-bromo-1,1-dimethylethyl)-naphthalene with  $\text{AgClO}_4$  and  $\text{LiAlH}_4$  (obtained as a 16:1 mixture by  $^1\text{H}$  NMR).<sup>4</sup> 2-(2-methyl-1-propen-1-yl)-naphthalene was prepared via Wittig reaction.<sup>5</sup>



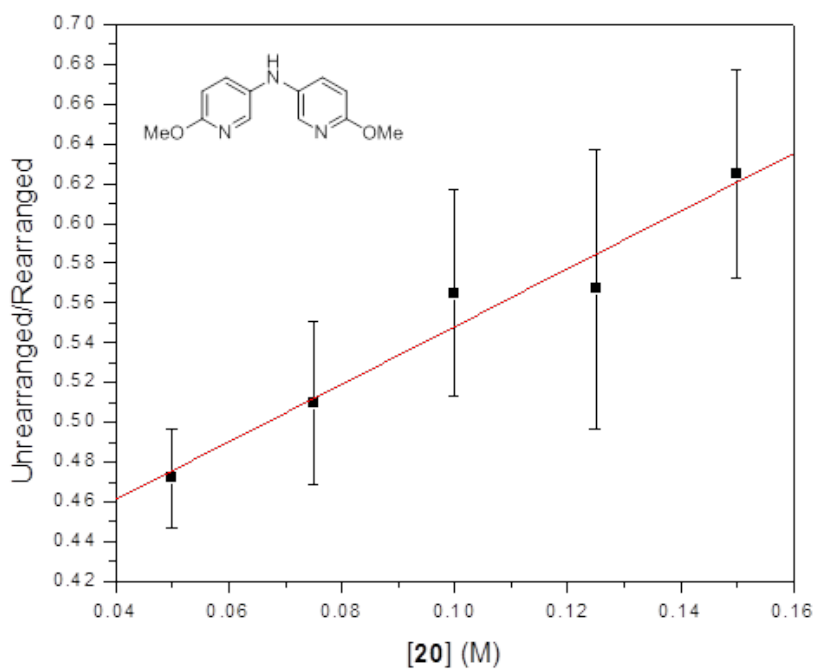
**Figure S53.** Plot used to obtain  $k_H = 1.3 \times 10^3 \text{ M}^{-1}\text{s}^{-1}$  for compound **2**.



**Figure S54.** Plot used to obtain  $k_H = 9.7 \times 10^2 \text{ M}^{-1}\text{s}^{-1}$  for compound **9**.

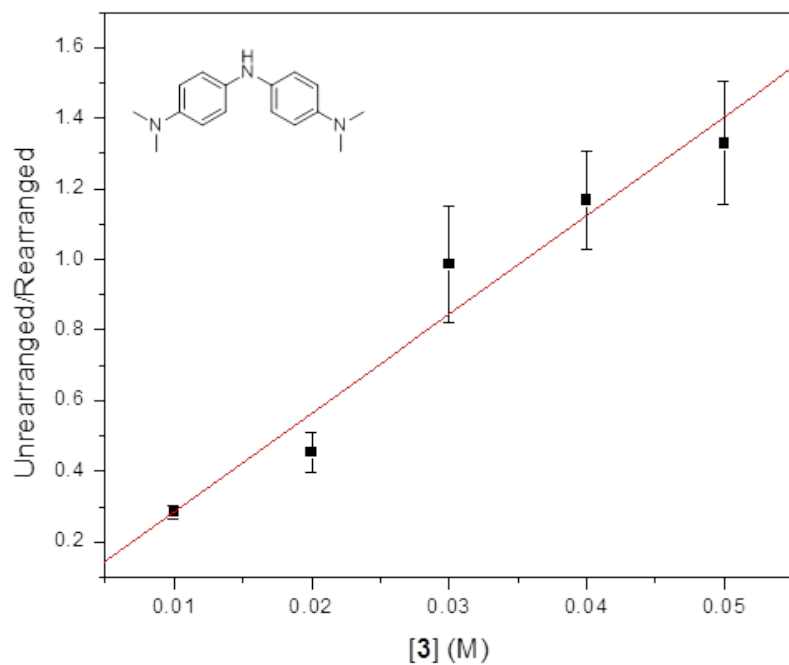


**Figure S55.** Plot used to obtain  $k_H = 2.5 \times 10^4 \text{ M}^{-1}\text{s}^{-1}$  for compound **17**.

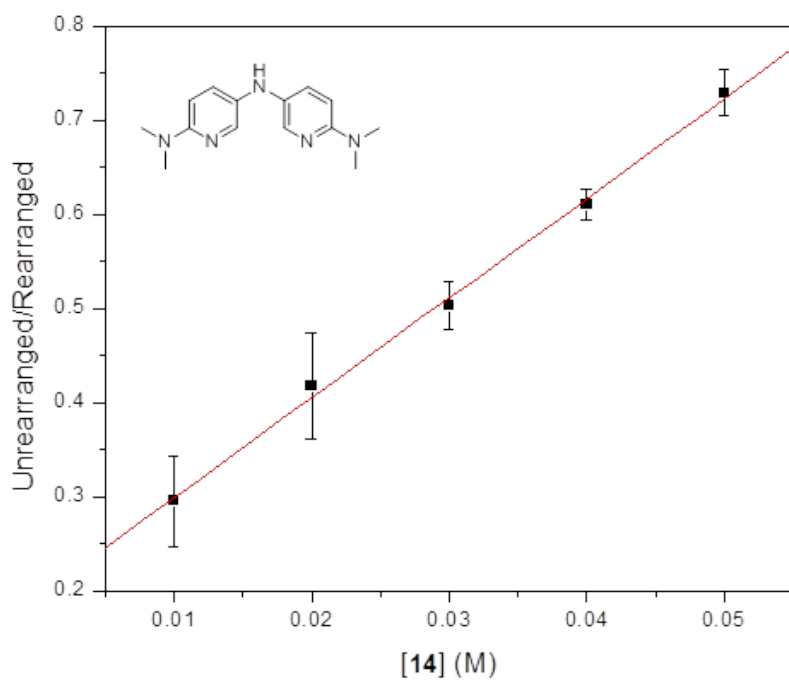


**Figure S56.** Plot used to obtain  $k_H = 2.0 \times 10^4 \text{ M}^{-1}\text{s}^{-1}$  for compound **20**.

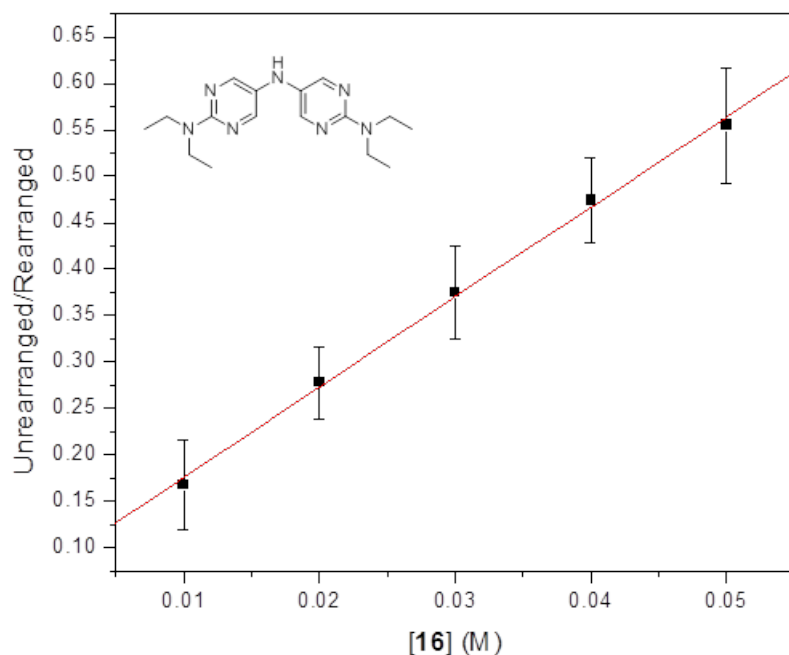




**Figure S57.** Plot used to obtain  $k_H = 3.2 \times 10^5 \text{ M}^{-1}\text{s}^{-1}$  for compound **3**.



**Figure S58.** Plot used to obtain  $k_H = 1.5 \times 10^5 \text{ M}^{-1}\text{s}^{-1}$  for compound **14**.

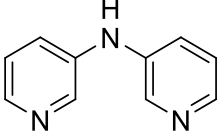
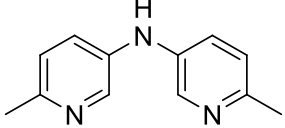
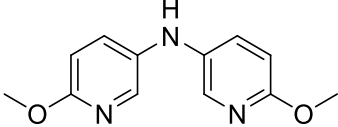
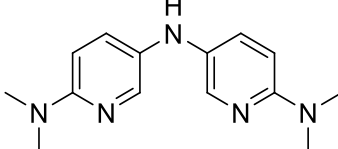
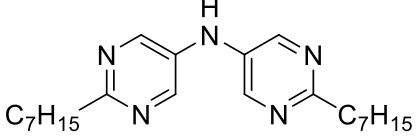
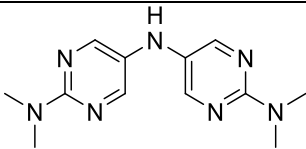
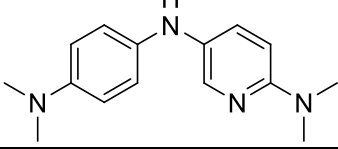
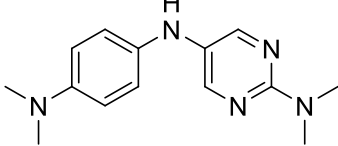


**Figure S59.** Plot used to obtain  $k_H = 1.4 \times 10^5 \text{ M}^{-1}\text{s}^{-1}$  for compound **16**.

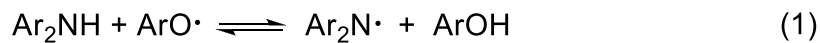
### BDE Measurements

EPR spectra were recorded at 298K in a Bruker Ellexsys 500 X-band spectrometer equipped with a standard temperature control unit, by irradiation of a solution of the diarylamine in benzene, containing 10% v/v di-*tert*-butyl peroxide, with the focused beam of a 500 W high-pressure Hg lamp, in the cavity of the spectrometer. Oxygen was removed by sparging with nitrogen. Radical equilibration experiments (REqEPR) were performed by continuous irradiation in the cavity of the EPR spectrometer of benzene solutions (containing 10% v/v di-*tert*-butylperoxide) of the diarylamine under investigation (1-50 mM) with a reference phenol (2-20 mM) in variable ratio. The equilibrium constant  $K_{eq}$  was then determined according to eq. 2 and used to determine the reaction  $\Delta G$  which yielded  $\Delta H$  under the assumption that the entropy change is negligible (eq. 3). Equilibrium constants are summarized in table S1, while examples of EPR spectra and corresponding simulation are reported in figures S60-S62.

**Table S1.** Experimental equilibrium constants measured by REqEPR and resulting BDE values for some diarylamines.

Diarylamine	Reference	$K_{eq}$	BDE (Kcal/mol)
	DBP	5.7±2.02	84.7±0.4
	DBP	65.0±23.1	83.1±0.4
	TBP	0.08±0.04	81.6±0.5
	TBP	4.60±1.9	78.8±0.8
	BHT	11.0±3.0	
	DBP	11.6±4.5	84.1±0.5
	TBP	4.5±2.6	79.2±0.5
	TBP	9.22±2.60	78.8±0.3
	TBP	6.10±3.05	79.0±0.5

**Legend:** reference (BDE). DBP: 3,5-di-*tert*-butylphenol (85.6 kcal/mol); TBP: 2,4,6-tri-*tert*-butylphenol (80.1 kcal/mol); BHT: 2,6-di-*tert*-butyl-4-methylphenol (79.9 kcal/mol). All BDEs are corrected for the revised value of phenol (-1.1 kcal/mol).<sup>7</sup>Reference (corrected) values for diphenylamine; 4,4' dimethyldiphenylamine; 4,4'-dimethoxydiphenylamine and 4,4'-dimethylaminodiphenylamine are: 84.7±0.7; 82.2±0.6; 80.7±0.3; 78.4±0.6 kcal/mol respectively.<sup>8</sup>



$$K_{eq} = \frac{\text{Ar}_2\text{N}\cdot}{\text{ArO}\cdot} \times \frac{\text{ArOH}}{\text{Ar}_2\text{NH}} \quad (2)$$

$$\Delta G = \Delta H - T\Delta S = RT \ln K_{eq} \quad (3)$$

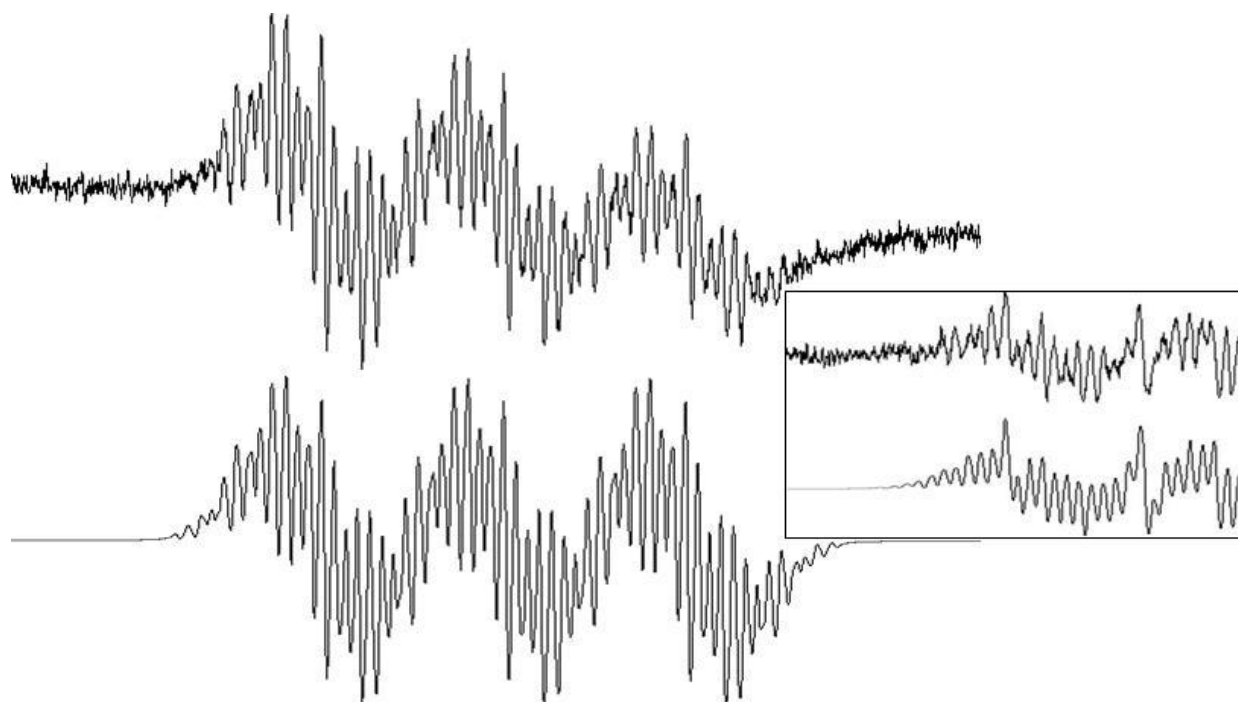


**Figure S60.** EPR spectrum recorded at 298 K by irradiating 3,3'-dipyridylamine in benzene containing 10% v/v di-*tert*-butylperoxide (top,  $g = 2.0040$ ) and its computer simulation (bottom) using the following spectral parameters:  $a(\text{N}) = 9.30$  G;  $a(2\text{N}) = 0.64$  G;  $a(2\text{H}) = 1.74$  G;  $a(2\text{H}) = 1.78$  G;  $a(2\text{H}) = 0.82$  G;  $a(2\text{H}) = 1.89$  G. Insert: low-field EPR portion of the spectrum obtained by irradiating a 1:1 mixture of the same compound with 3,5-di-*tert*-butylphenol and its computer simulation for a radical ratio (diarylaminy/phenoxyl) of 100:8.4.

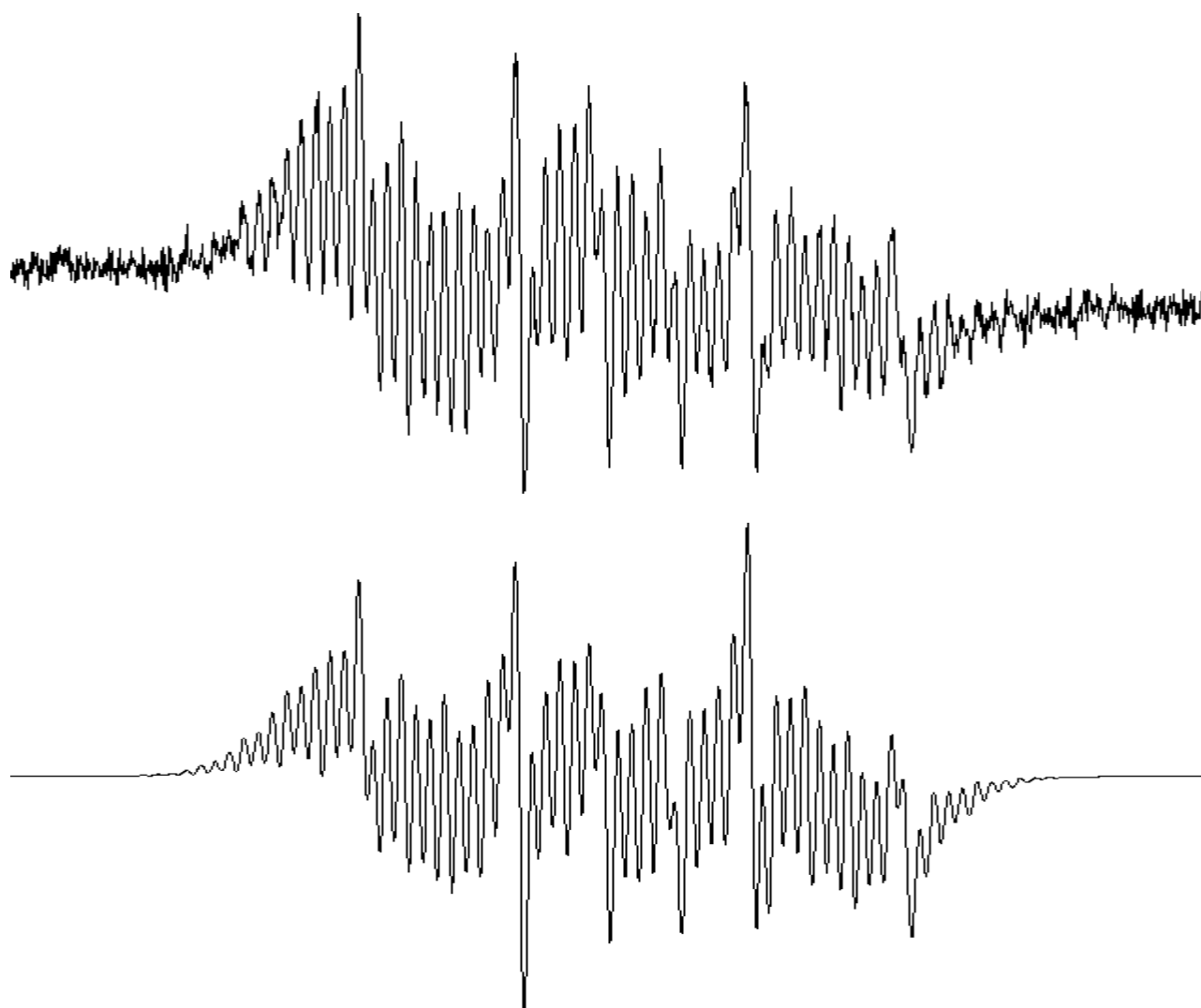


**Figure S61.** EPR spectrum recorded at 298 K by irradiating a mixture of **9** and 3,5-di-*tert*-butylphenol in molar ratio 1:3.5 (top), and simulated spectrum with a ratio of 100:6.3 between the corresponding radicals (bottom). Simulation has been obtained with the following parameters  $\text{Ar}_2\text{N}\cdot$ :  $a(\text{N})$  8.95G;  $a(2\text{N})$  0.56 G;  $a(2\text{H})$  0.7 G;  $a(2\text{H})$  1.71G;  $a(2\text{H})$  1.83G;  $a(6\text{H Me})$  1.97 G. (center difference – 1.27 G- $\rightarrow$   $g=2.0040$ );  $\text{ArO}\cdot$ :  $a(\text{H})$  10.3G;  $a(2\text{H})$  6.69G;  $a(18\text{H})$  ca. 0.1G ( $g=2.0048$ ).

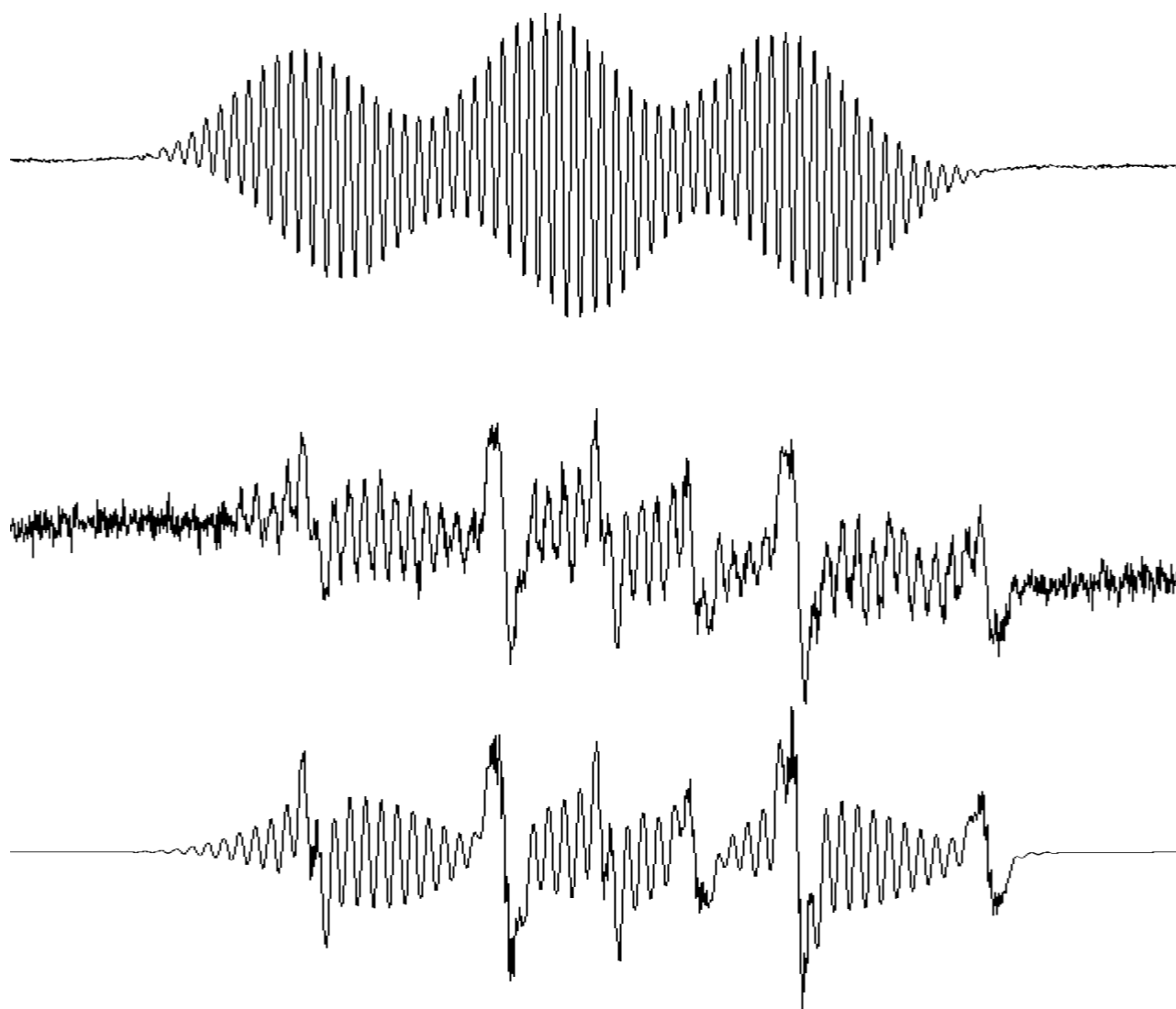


**Figure S62.** EPR spectrum recorded at 298 K by irradiating benzene/di-*tert*-butylperoxide containing **11** alone (top), in mixture with 3,5-di-*tert*-butylphenol in molar ratio 1:1 (middle), and simulated spectrum with a ratio of 100:38 between the corresponding radicals (bottom). Simulation has been obtained with the following parameters  $\text{Ar}_2\text{N}^\bullet$ :  $a(\text{N})$  8.57G;  $a(4\text{N})$  0.55G;  $a(4\text{H})$  1.59G;  $a(4\text{H hept})$  2.14 G;  $a(4\text{H hept})$  0.12G;  $\text{ArO}^\bullet$ :  $a(\text{H})$  10.3G;  $a(2\text{H})$  6.69G;  $a(18\text{H})$  ca. 0.1G.

## References

- (1) Hanthorn, J. J.; Pratt, D. A. *J. Org. Chem.* **2012**, *77*, 276.
- (2) Jha, M.; Pratt, D. A. *Chem. Commun.* **2008**, 1252.
- (3) Leardini, R.; Lucarini, P.; Pedulli, G. F.; Valgimigli, L. *J. Org. Chem.* **1999**, *64*, 3726.
- (4) Shimizu, N.; Watanabe, K.; Tsuno, Y. *Chem. Lett.* **1983**, 1877.
- (5) Kraus, G. A.; Choudhury, P. K. *Synlett* **2004**, 97.
- (6) Hanthorn, J. J.; Valgimigli, L.; Pratt, D. A. *J. Am. Chem. Soc.* **2012**, *Articles ASAP*. DOI: 10.1021/ja30086z
- (7) Mulder, P. Korth, H.-G.; Pratt, D. A.; DiLabio, G. A.; Valgimigli, L.; Pedulli, G. F.; Ingold, K. U. *J. Phys. Chem. A* **2005**, *109*, 2647-2655
- (8) a) Lucarini, M.; Pedrielli, P.; Pedulli, G. F.; Valgimigli, L.; Gigmes, D.; Tordo, P. *J. Am. Chem. Soc.* **1999**, *121*, 11546-11553; b) Pratt, D. A.; DiLabio, G. A.; Valgimigli, L.; Pedulli, G. F.; Ingold, K. U. *J. Am. Chem. Soc.* **2002**, *124*, 11085.